CHALMERS
UNIVERSITY OF TECHNOLOGY

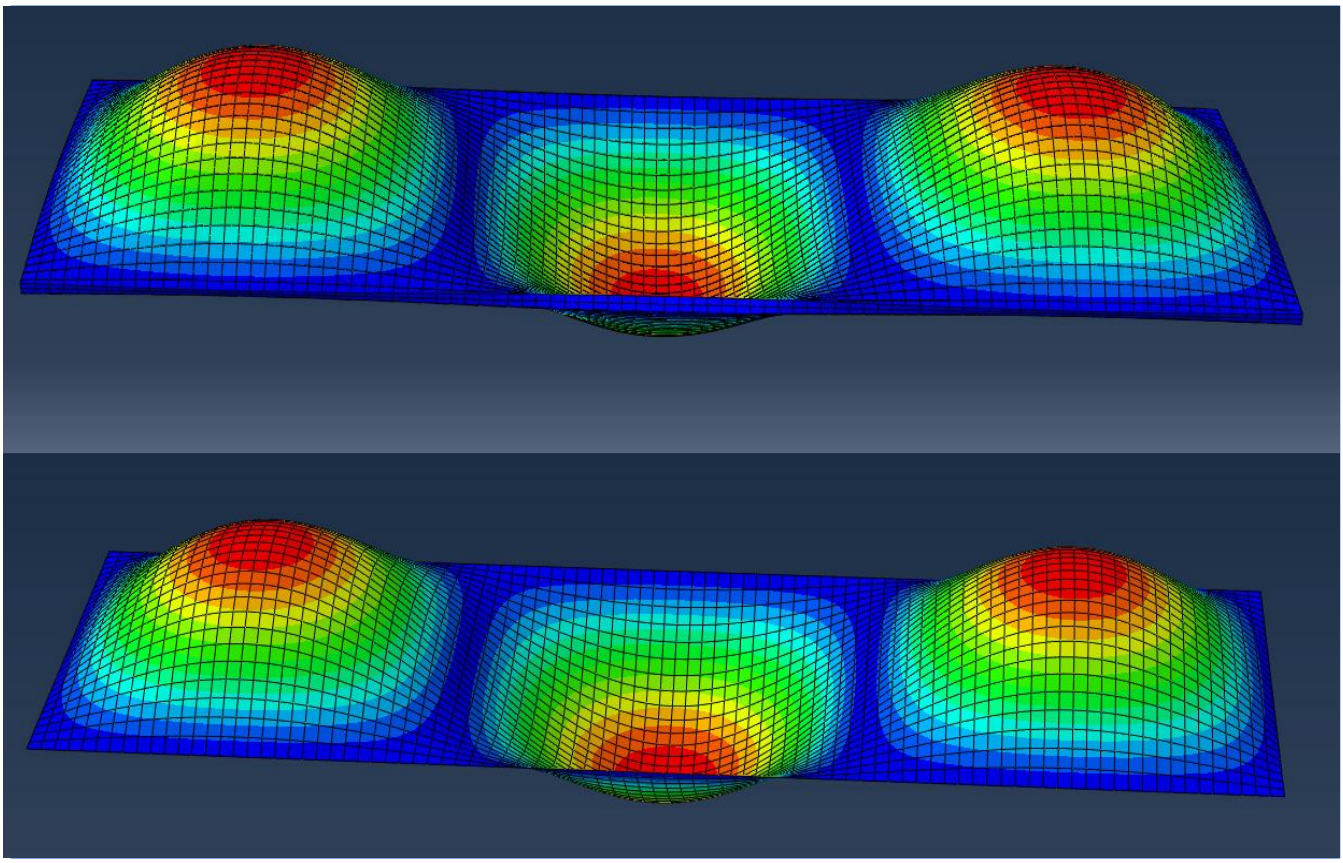

Buckling Analysis of Orthotropic Plates

Stiffened plate and steel sandwich plates

Master's Thesis in the Master's Programme Structural Engineering and Building Technology

JÓN PÉTUR INDRIÐASON
VÉSTEINN SIGMUNDSSON

Department of Civil and Environmental Engineering
Division of Structural Engineering
Steel and Timber Structures
CHALMERS UNIVERSITY OF TECHNOLOGY
Gothenburg, Sweden 2015
Master's Thesis 2015:79

MASTER'S THESIS 2015:79

Buckling Analysis of Orthotropic Plates

Stiffened plate and SSP

Master's Thesis in the Master's Programme Structural Engineering and Building Technology

JÓN PÉTUR INDRIÐASON

VÉSTEINN SIGMUNDSSON

Department of Civil and Environmental Engineering

Division of Structural Engineering

Steel and Timber Structures

CHALMERS UNIVERSITY OF TECHNOLOGY

Göteborg, Sweden 2015

Buckling Analysis of Orthotropic Plates
Stiffened plates and SSP

Master's Thesis in the Master's Programme Structural Engineering and Building Technology

JÓN PÉTUR INDRIÐASON

VÉSTEINN SIGMUNDSSON

Examensarbete 2015:79/ Institutionen för bygg- och miljöteknik,
Chalmers tekniska högskola 2015

Department of Civil and Environmental Engineering
Division of Structural Engineering
Steel and Timber Structures
Chalmers University of Technology
SE-412 96 Göteborg
Sweden
Telephone: + 46 (0)31-772 1000

Cover: Shows the buckling of a sandwich panel as a full 3D model and an equivalent 2D model. This analysis can be found in chapter 5.2.

Chalmers reproservice / Department of Civil and Environmental Engineering Göteborg, Sweden, 2015

Buckling Analysis of Orthotropic Plates
Stiffened plate and SSP

Master's thesis in the Master's Programme Structural Engineering and Building Technology

JÓN PÉTUR INDRIÐASON
VÉSTEINN SIGMUNDSSON
Department of Civil and Environmental Engineering
Division of Structural Engineering
Steel and Timber Structures
Chalmers University of Technology

ABSTRACT

Sandwich plate referred to as SSP is a combination of two face sheets of high stiffness and a less stiff core which together give a high strength to weight ratio. In the first half of the 20th century a great demand for such a structure arose in the ship and aviation industry. This demand increased research of the sandwich concept which quickly became a desirable concept for the civil industry, especially in bridge design. Since the concept was first introduced many papers have been published concerning the concept with various topics, especially fatigue, bending and deflection. Buckling, which is this papers main subject, has not been addressed as much.

The purpose of this master's thesis was to research different analytical and modelling methods for analysis of buckling of orthotropic plates. What different assumptions and simplifications are made and how they are compatible. The objective of this research was to study the design process of orthotropic plates with respect to buckling.

The literature study begins by going through the general concepts of buckling analysis in the context of a simple plate before going into more complex stiffened plate and SSP. After discussing the theory, the existing models and theories where compared including analytical methods, finite element models and existing freeware programs such as EBPlate. Because of the complex geometry and behaviour of the sandwich plate the stiffened plate was studied first with the aim of using similar methodology in design for the sandwich plate.

In the buckling analysis of the stiffened plate, five different methods where compared. The methods were found to give very similar results. In section 4 the analysis of the stiffened plate can be found and seen how well they correlated. In the SSP analysis four different methods where used and compared. The methods were tested with three panels and all three panels where tested with 6 different cross-sections. For plate like behaviour the tests where positive but for column like behaviour the analytical method and EBPlate did not correlate to the finite element models. An unexpected drop in critical buckling stress was encountered when the web thickness was increased in both FEM models which is suggested to be explored in future studies.

The conclusion was that EBPlate proved to be an easy and accurate tool to use for the stiffened plate. In the attempts to manipulate EBPlate to be applicable for SSP a good

correlation was found between the more complex finite element models for plate like behaviour. It is clear from this results that EBPlate could be a handy tool for designers especially in preliminary design but for the final design a more thorough 3D FEM analysis might need to be performed.

Key words: Critical buckling stress, SSP, Stiffened plate, ABAQUS, EBPlate, Sandwich plate.

Content

Preface

In this study, a thorough literature study on the subject of buckling of orthotropic plates is conducted to learn the predicted behaviour of both stiffened plates and sandwich plates. Furthermore, published analytical models, FE-modelling in 2D and 3D are applied to a number of panels and compared. EBPlate is a freeware program that is made primarily for stiffened plate but was altered to be applicable for sandwich panels.

This project is a part of many on the subject of SSP focusing on buckling and was carried out by the authors with the explicit help of the supervisor and examiner Mohammad Al-Emrani. The project research and modelling was all carried out in the department of structural engineering at Chalmers.

Co-workers of ours that have been a great deal of help are a number of people, Peter Nilsson graduate student at the department was to a great help during the modelling process, David and Walter who derived Libove and Hubka equations gave us access to them for use and finally our opponents, Guðlaugur Már Guðmundsson and Óskar Bragi Guðmundsson, gave us a helping hand all along the study.

Göteborg June 2015

Jón Pétur Indriðason & Vésteinn Sigmundsson

1 Introduction

1.1 Background

Today most bridge decks are made using orthotropic plates consisting of a stiff face sheet that are stiffened with stiffeners referred to as ribs. The idea behind stiffened plates is to increase strength by adding stiffeners instead of increasing the plate thickness. The stiffeners can be of an open or closed type where the closed type offers a lot better torsional stiffness than the open one and is therefore more common. The problem with these bridge decks is that they have a relatively short life expectancy because of fatigue. The welds that are needed to attach the stiffeners to the face sheet do not handle fatigue load for long. (Guo Tong, Li Aiqun, & Li Jianhui, 2008) conducted a survey which revealed that 80-90% off failure in steel structures is fatigue and fracture.

A better alternative is the SSP which is working its way into the bridge industry today. The SSP offers better abilities then the stiffened plate on all fronts. The SSP has a significant increase in high strength-to-weight ratio compared to the stiffened plate. Its limitation that hindered mass development was for a long time the production time which was too long because of lack of laser welding technology. With the discovery and development of the hybrid laser arc welding HLAW which is a fast and efficient, SSP has really become a viable option. This laser-weld has a lot better performance with respect to fatigue as well as being much faster than before(Kolsters & Zenkert, 2009).

The sandwich plate concept is not a recently discovered structural element, it was introduced a while ago in the field of aerodynamics and ship building. At the time when airplanes were being designed into the form we know them today, in the first half of the last century. A need for light weight and high stiffness structure was needed which encouraged the development of the SSP which has a particularly high strength to weight ratio. In the 1980´s ship building industry's started experimenting with laser welding to improve production quality and time efficiency which was its biggest problem.

Sandwich steel plates are always a combination of two thin, high strength plates, a top flange and a bottom flange and a less stiff web in-between. The core of the plate acts as a longitudinal stiffener giving the plate different stiffness and stretching abilities in different directions. For the civil engineering application a number of papers have been published concerning research of the SSP concept ((Kolsters & Zenkert, 2009),(Galéa & Martin, 2010)). In these papers a lot of different configurations of the core are analysed with respect to deflections, bending capacity(Chang, Ventsel, Krauthammer, & John, 2005) and, the one particularly interesting for this master thesis, buckling analysis(Galéa & Martin, 2010)(Kolsters & Zenkert, 2009).

1.2 Project aim

The aim of this master's thesis is to explore global buckling behaviour of orthotropic plates. Different analytical and numerical modelling methods for both stiffened plate and SSP will be compared and their result compared. The end result

should be a simplification of designing orthotropic steel panels with respect to buckling.

1.3 Method

The master thesis starts with a thorough literature study of the basic concept of buckling of plate and column and the differences in behaviour between these two, i.e. the post critical strength and how these two types of behaviour interact. By grasping the basic theory well with respect to boundary conditions, effective area and all the important concepts the authors thought to be crucial to comprehend explicitly before attempting to analyse the more complex behaviour of an orthotropic plate.

The literature study then moves on to the orthotropic plates starting with the stiffened plate where two different analytical methods are considered in detail. More analytical methods exist and where considered but not included in the final work. The first study is the simplest analytical method from Annex A1 of EN 1993-1-5. A more precise analytical method based on a modified Euler buckling formula derived by Timoshenko and published in (Hughes, Ghosh, & Chen, 2004) is studied next. In that method a more precise analysis of stiffened plate is covered where global buckling is considered taking transverse shear into account which is neglected in EC 1993-1-5.

After the literature study the modelling and verification for both the stiffened plate and the SSP follows. In both analysis 3D finite element models were made and used as a base meaning that it was considered to yield the most accurate results but at the same time the most time consuming and computationally heavy. All analytical models, EBPlate and the 2D equivalent model, used in the SSP analysis, have some approximations that limit the result to some degree. How much difference is between these models is the interesting thing that was the objective of the master's thesis.

Before running the critical buckling analysis of the SSP, the finite element models had to be verified to see that they had been modelled correctly and were behaving as they should. Since no published work where critical buckling analysis are mode on SSP, the models had to be verified with respect to something else. It was decided to verify the models with respect to deflection since a number of papers have been published on that subject and therefore a number of verified models to compare to.

1.4 Outline

The first chapter is a general introduction and an overview of the master thesis which sets the tone for work within. Following the first chapter is the literature study which is threefold, starting with a general buckling study going from a simple column to a plate with plate like behaviour. The second and third parts of the literature study are the stiffened plate and SSP respectively. In the stiffened plate chapter the analytical methods that will be tested are discussed. In the SSP chapter there is a more thorough discussion about the structure and behaviour of SSP. Then the stiffness parameters are discussed and how they are applied in the

analysis as a 2D equivalent plate. A small discussion on the 3D modelling and possible sources of errors before ending with the analytical method used in the analysis.

Chapter three is all about the freeware program EBPlate its methodology and calculation methods. How the program takes the stiffeners into account in two different ways and how it handles local and global buckling. In the final subchapter it is discussed how the program can be manipulated to be applicable for SSP analysis.

Chapters 4 and 5 go through the real analysis done on the stiffened plate and the SSP respectively. In them first the different methods are discussed and in the end the results of all the methods are compared and concluded from the results.

In chapter 6 the final conclusions for the master thesis are put forth for both the stiffened plate and the SSP and discussed how the results can help in design of orthotropic plates in general.

Finally, there is the discussion chapter where the overall results are discussed and future work proposed on the subject.

1.5 Limitations

Limitation made in the stiffened plate analysis are the following

- Only Simply supported edge conditions are considered
- Open ribs only
- The plates were designed such that local buckling is not the decisive mode of instability. Thus only global buckling is studied
- Only unidirectional edge compression is considered in the analysis

The same limitations apply for the SSP analysis. In addition, only

- V-shaped corrugated web only

2 Literature study

2.1 Introduction

This chapters contain all the basic concepts and theories used for calculation of critical buckling stress of three different plate types. The first subchapter is about phenomenon called column buckling, column-like plate buckling and plate buckling where concepts such as elastic stress and buckling coefficient are explained. The second subchapter is about stiffened plates and contains analytical solutions of critical buckling stress. Two different analytical approaches are explained where pros and cons of each method are described. Finally, the third subchapter takes care of sandwich plates and will contain the theories behind the sandwich concept and the methodology applied in the following modelling chapter.

2.2 Column-like plate buckling and Plate Buckling

2.2.1 General introduction

Buckling is a mode of failure in which there is a sudden out of plain deformation of a member under compression. The phenomenon can occur when the compressive forces or stresses become higher than a certain critical value which might happen even though the yield strength of the steel has not yet been reached. The pressure can be caused by many different load cases, for example, bending moment, shear or local concentrated load in the transversal direction. Sometimes it can also be a combination of two or more load cases.

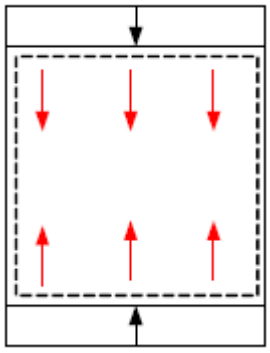

Figure 2.1. Supported plate under compression

Plates under uniaxial compression as shown in Figure 2.1 could have one of two different types of buckling mode, global buckling and local buckling. A combination of the two can also happen simultaneously in a plate. Mode interaction can cause a significant decrease in the load-carrying capacity. Local buckling can be explained as: when a cross-section under compression/shear for a plate element fails before overall column failure or overall plate failure happens. One the other hand, global buckling occurs when a whole cross-section under compression or shear for a plate fail as an overall plate failure. The difference between plate buckling and column buckling is defined in the boundary conditions. For plate buckling to occur the plate must have three or more edges supported while column buckling has only two edges supported.

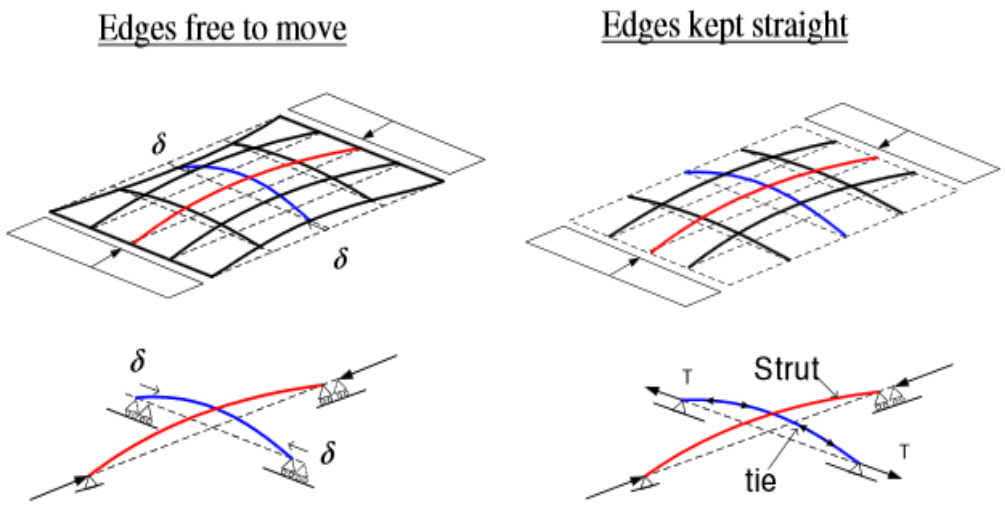

Figure 2.2 Plate support on two edges vs plate with support on all edges

When plate is supported on all the edges the plate gets higher critical buckling stress due to redistribution of stresses from the middle of the plate to the edges. Figure 2.2 describes how a plate supported on all four edges acts when the axial pressure is increased. Initially the plate starts to buckle where the stiffness is lowest and for a plate supported on all edges it happens in the middle. From there it gradually buckles more and more towards the sides losing more and more stiffness. Finally, the plate has no more stiffness and the buckles. The last plate in figure 2.3 shows a simple strut and tie model and explains how the post-critical strength for a plate works as the middle part wants to buckle but is prevented because of the edges.

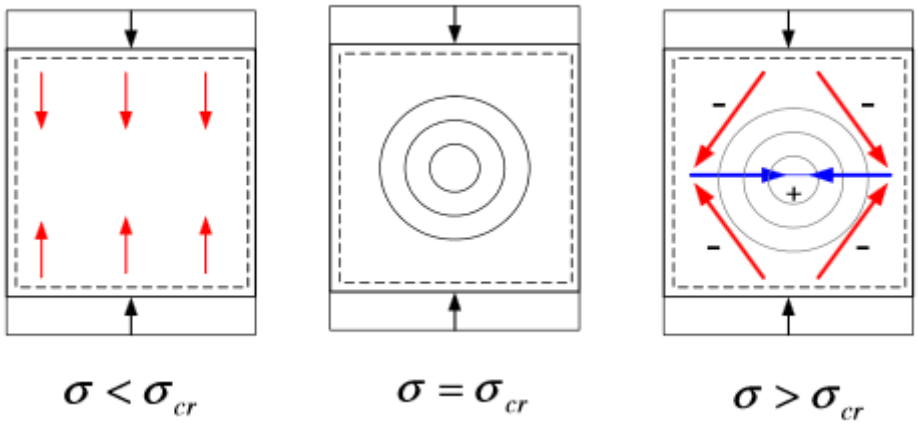

Figure 2.3. Plate supported on all four edges under compression on two edges develops post-critical buckling strength.

The aspect ratio of the plate can also play part when it comes to buckling. Sometimes fracas like “plate-like behaviour” and “column-like behaviour” are used to describe the buckling mode of a plate. The difference lies in the ratio between the length (a) and the width of the plate (b), i.e. the plate aspect ratio. For

example, plates with low aspect ratios (a>b) has more "column-like" behaviour than "plate-like" behaviour with no or very limited post-critical strength. Therefore, the critical buckling stress can be estimated from that of a column. On the other hand, when the ratio is higher (around one or higher) the edges contribute more and the critical buckling stress is similar as a plate with more post-critical strength.

2.2.2 Column buckling

For a pinned-pinned column under compression the critical buckling stress can be obtained from:

$$\sigma_{cr} = \frac{n^2 \pi^2 EI}{AL^2} \qquad (2.1)$$

Where:

σ_{cr}	critical buckling stress
E	elastic modulus
I	moment of inertia for the cross-sectional area
n	number of sinus curves
A	area of the column
L	length of the column

2.2.3 Column like buckling of a plate

According to Euler theory, the critical buckling load for strut or a plate supported only on two edges can be obtained with equation (2.2).

$$P_{cr} = \frac{\pi^2 EI}{a^2} \frac{1}{(1-\nu^2)} \qquad (2.2)$$

Where:

P_{cr}	critical buckling load
a	length of the column
ν	Poisson's ratio

This expression assumes that a "plate strut" has relativity large width compared to the (buckling) length of the strut. Therefore, the free strain deformation in the transverse direction in the centre of the plate compared to the support edges needs to be taken into account. The second quotient of the equation (2.2) (1/ (1-ν^2)) takes this into account.

After that, the critical buckling load can be found by dividing the critical load with the steel plate area. Hence, the critical buckling stress for a strut or a column supported on two edges under an axial load can be obtained from:

$$\sigma_{cr} = \frac{\pi^2 E}{12(1-\nu^2)\left(\frac{a}{t}\right)^2} \qquad (2.3)$$

2.2.4 Plate buckling

As mentioned before, plate buckling is defined by having at least three or more edges fixed. The buckling effect is quite different when the plate is fixed on more than two edges. Buckling coefficient k is introduced and the critical buckling stress becomes a function of width rather than of length. Furthermore, when dealing with plates with aspect ratios larger than 1,0 the length becomes irrelevant but instead the width becomes the determining factor for buckling strength. The key effect that explains the change in behaviour is the post-critical strength.

The definition of a plate behaviour can be described with an example for a plate supported on all four edges and loaded with uniformly distributed axial load on two edges. When the plate starts to deform in the transversal direction an additional force is needed to keep the plate in its deformed shape otherwise the plate would return to its original form. Hence, the transvers force needs to be in balance with the re-bouncing force.

To understand the concept of critical buckling stress in a steel plate one has to study the differential equation for plate obtained from:

$$D\left(\frac{\delta^4\omega}{\delta x^4}+2\frac{\delta^4\omega}{\delta x^2\delta y^2}+\frac{\delta^4\omega}{\delta y^4}\right)=q \qquad (2.4)$$

Where D describes the bending stiffness of the plate,

$$D=\frac{Et^3}{12(1-\nu^2)} \qquad (2.5)$$

Now the load is not applied in axial direction, instead it is applied in the transvers direction as shown in Figure 2.4.

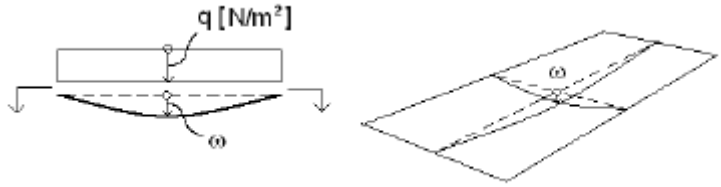

Figure 2.4. Deflection of a two-way plate

Than the differential equation for loaded plan becomes:

$$D\left(\frac{\delta^4\omega}{\delta x^4}+2\frac{\delta^4\omega}{\delta x^2\delta y^2}+\frac{\delta^4\omega}{\delta y^4}\right)=\sigma_{cr}t\frac{\delta^2\omega}{\delta x^2} \qquad (2.6)$$

Where the general solution is as following,

$$\omega=Asin\left(\frac{m\pi x}{a}\right)sin\left(\frac{n\pi y}{b}\right) \qquad (2.7)$$

Where:

A	constant
m	number of half-sinus waves in the longitudinal direction
n	number of half-sinus waves in the transverse direction
a	length of the plate
b	width of the plate
ω	out-of-plane deflection

Combination of equation (2.6) and equation (2.7) gives:

$$\sigma_{cr} = \frac{\pi^2 D a^2}{t m^2}\left(\frac{m^2}{a^2} + \frac{n^2}{b^2}\right)^2 \qquad (2.8)$$

The lowest value for critical buckling stress is when n=1. Then the transvers direction has only one half-sine wave. Hence, the critical buckling stress for a plate can be obtained from:

$$\sigma_{cr} = k\frac{\pi^2 E}{12\cdot(1-\nu^2)\cdot\left(\frac{b}{t}\right)^2} \qquad (2.9)$$

Where:

σ_{cr}	critical buckling stress
k	buckling coefficient
E	Elastic modulus
t	plate thickness
b	width of the plate
ν	Poisson's ratio

Buckling coefficient k is a function of the ratio between the length a and the width as well as the number of half-sine wave's m in the longitudinal directions. It can be obtained from:

$$k = \left(\frac{mb}{a} + \frac{a}{mb}\right)^2 \qquad (2.10)$$

For a plate supported on all edges where the aspect ratio between length and width is around one, two or three (a/b=1, 2 ,3…), the buckling coefficient will have the lowest value and therefore yields the lowest possible result for critical buckling stress as shown in Figure 2.5. On the other hand, for plates that are short and wide, higher buckling coefficient is gained that leads to higher critical buckling stress. Therefore, aspect ratio of the plate plays big part when it comes to calculation of critical buckling stress. Also, loading and boundary conditions have great influence on the buckling behaviour and critical buckling stress. More fixation on edges will cause more stiffness which in turn increase the buckling load of the plate.

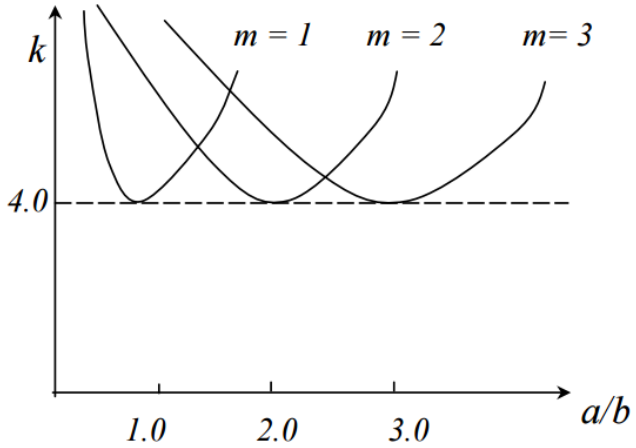

Figure 2.5. Buckling coefficient as function of the aspect ratio a/b for simply supported plate

2.3 Stiffened plate (Orthotropic)

2.3.1 General introduction

Stiffened plates have been around for a long time and were for the longest time the only way of adding stiffness to steel plates effectively. Why the stiffened plate was invented is for a more effective use of material. Instead of increasing the plate thickness the same result can be achieved using stiffeners. There exist many variations of stiffeners such as simple I-stiffener, T-stiffener and closed stiffener, see Figure 2.6. All the stiffeners have in common that they add stiffness in their parallel direction but the T-stiffener and the closed stiffener provide torsional stiffness as well to an extent that must be taken into account. In this master thesis the normal I-stiffeners is the only one that is taken into account.

In design of stiffened plate or plate girders one of the most important checks is the buckling check where correct design procedure can save material and production cost. In order to do so for longitudinally stiffened plates or plate-girders subjected to edge compression two effects must be taken into account which are the plate-like-behaviour and the column-like-behaviour as was discussed in the previous chapter. For analysis of the former type of behaviour the critical buckling stress is required. For this reason, the main objective of this master thesis is to estimate the critical buckling stress for plate-like-behaviour.

In this chapter two analytical methods for estimating the critical buckling stress for stiffened plates are discussed. The first one is how Eurocode deals with the calculations in Annex A from EN-1993-1-3. The second analytical model is the modified Euler buckling formula which we will refer to as “Modified Timoshenko method”. This method is a more accurate method because torsional stiffness of the stiffened plate is taken into account which otherwise is neglected in the Eurocode method.

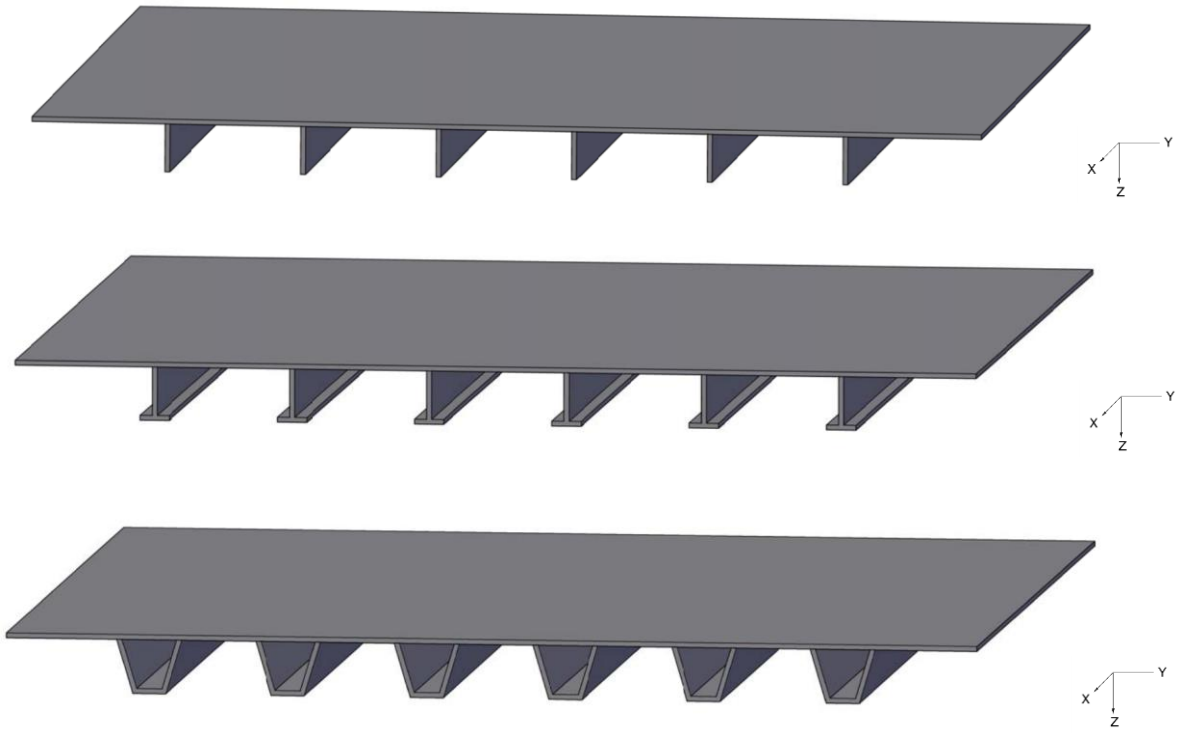

Figure 2.6. Variations of stiffeners, from top, I-stiffener, T-stiffeners and closed-stiffener.

2.3.2 Annex A from EN1993-1-3

Eurocode 1993 -Annex A gives an approximation method for estimating the elastic critical buckling stress for a plate supported on three or more edges. This analytical method should be used with precaution since it neglects some favourable effects, such as stiffeners placed in the tension zone of the plate. Another disadvantage with this method is that even though it gives rather good results for stiffened plate with one stiffener or with three stiffeners or more, when it comes to a plate with two stiffener the method can give inconsistent results (Galéa & Martin, 2010). In the work conducted in this thesis, plates will only be tested in compression and all plates will have at least six stiffeners or more. In addition, since only flat stiffeners will be included in the analysis neglecting the torsional stiffness will not result in major error.

According to the model in Annex A of EN 1993-1-5, the elastic critical buckling stress can be calculated from:

$$\sigma_{cr,p} = \kappa_{\sigma,p}\sigma_E \qquad (2.11)$$

Where:

$\sigma_{cr,p}$ critical buckling stress of a panel
$\kappa_{\sigma,p}$ buckling coefficient
σ_E elastic critical buckling stress

The elastic critical buckling stress can be obtained from:

$$\sigma_E = \frac{\pi^2 E t^2}{12(1-\nu^2)b^2} \quad (2.12)$$

Where:

E elastic modulus
ν Poisson's ratio
b width of the plate
t thickness of the panel

The buckling coefficient for an orthotropic plate with smeared out stiffeners over the panel can be obtained from:

$$if\ \alpha \leq \sqrt[4]{\gamma} \quad \kappa_{\sigma.p} = \frac{2((1+\alpha^2)^2 + \gamma - 1)}{\alpha(\psi+1)(1+\delta)} \quad (2.13)$$

$$if\ \alpha > \sqrt[4]{\gamma} \quad \kappa_{\sigma.p} = \frac{4(1+\sqrt{\gamma})}{(\psi+1)(1+\delta)} \quad (2.14)$$

$$\psi = \frac{\sigma_2}{\sigma_1} \quad (2.15)$$

$$\gamma = \frac{I_{sl}}{I_p} \quad (2.16)$$

$$\delta = \frac{\sum A_{sl}}{A_p} \quad (2.17)$$

$$\alpha = \frac{a}{b} \quad (2.18)$$

Where:

ψ stress distribution
γ flexural stiffness of stiffener
δ relative axial stiffness
α aspect ratio of the plate

I_{sl} second moment of area for the hole plate

I_p second moment of area for bending of the plate $= \frac{Bt^3}{12(1-\nu^2)}$

$\sum A_{sl}$ sum of the gross areas of the individual longitudinal stiffener

A_p gross area of the plate $= bt$

σ_1 larger stress

σ_2 smaller stress

a length of the plate

b width of the plate

2.3.3 Modified Euler buckling formula (Timoshenko)

Another analytical method based on modified Euler buckling formula (Timoshenko) is introduced in (Hughes, Ghosh, & Chen, 2004) and can be used for estimating the elastic critical buckling stress of a panel. The method has been modified for better analytical solution for global buckling of stiffened panels for the ship industry. The advantage of this method compared with the one described in chapter 2.3.2 is that it takes into account factors that are neglected in Annex A from En1993-1-5 such as,

- Transverse shear that causes an additional deflection that leads to reduced overall buckling stress
- More accuracy when it comes to calculation of the panel geometric properties.

When it comes to calculation of the overall panel buckling, the size of the stiffeners controls how the analytical solution for critical buckling is described. It is important when choosing an analytical solution to distinguish between a lightly stiffened plate and heavily stiffened plate. Few guidelines have been established to identify lightly stiffened plates based on the geometric properties. The virtual aspect ratio of an orthotropic plate is described by the size of the panel and the stiffness of the plate and can be obtained from:

$$\Pi_0 = \left(\frac{a}{B}\right)\left(\frac{D_y}{D_x}\right)^{\frac{1}{4}} \qquad (2.21)$$

Where:

a length of the plate

B width of stiffened panel

D_y flexural rigidity of orthotropic plate in y-direction $\left(= \frac{EI_y}{a}\right)$

I_y moment of inertia for the length of the plate $\left(= \frac{at^3}{12}\right)$

When the virtual aspect ratio is small the stiffeners become independent and the panel will buckle like a column. There are several ways in which the virtual aspect ratio can be small:

- If the bay is short or wide(small a/B)
- If stiffeners are heavy (large D_x)
- If the plate is thin (small D)
- If spacing between stiffeners is small(small b)

The analytical solution for an overall buckling for a lightly stiffened plate is given by:

$$\sigma_{ov,orth} = \frac{\pi^2 D_x}{a^2 t} k_{orth} \qquad (2.19)$$

Where:

t thickness of the plate

D_x flexural rigidity of orthotropic (stiffened) plate in x-direction $\left(= \frac{EI_x}{b_{stiff}}\right)$ (see Figure 2.6)

I_x Moment of inertia of a single stiffener plus the attach plating between stiffeners.

b_{stiff} width between the stiffeners

The buckling coefficient can be obtained from:

$$k_{orth} = 1 + 2\eta\Pi_0^2 + \Pi_0^4 \qquad (2.20)$$

For the orthotropic torsional stiffness parameter:

$$\eta = \frac{H}{\sqrt{D_x D_y}} = \frac{H}{\sqrt{D_x D}} \qquad (2.22)$$

Where:

H torsional rigidity of orthotropic plate $\left(= \left(\frac{1}{6Gt^3} + \frac{GJ_x}{b}\right)\right)$

G shear modulus $\left(= \frac{E}{2(1+\nu^2)}\right)$

D flexural rigidity of isotropic plate $\left(= \frac{Et^3}{12(1-\nu^2)}\right)$

E elastic modulus

ν Poisson's ratio

J_x torsional rigidity of a longitudinal stiffener for continuous stiffening $\left(= \frac{1}{6}(h_w {t_w}^3 + b_f {t_f}^3)\right)$

Until now the focus has been on describing the analytical solution for a lightly stiffened plate. For cases were the stiffeners are considered large the critical overall buckling stress can be obtained from:

$$\sigma_{ov.panel} = \sigma_E \left(\frac{A_w G}{A_w G + A_T \sigma_E} \right) k_{orth} \qquad (2.23)$$

Where the Euler buckling stress for a column like behaviour is obtained from:

$$\sigma_E = \frac{\pi^2 E}{\left(\frac{a}{\rho}\right)^2} \qquad (2.24)$$

Where:

ρ is the radius of gyration of longitudinal stiffener with attached plating $\left(= \frac{\sqrt{I_x}}{A_T}\right)$

The part inside the parentheses in equation (2.23) takes into account the transverse shear due to a slope of a column and is descripted by Timoshenko (Timoshenko, 1936). This transvers shear causes an additional deflection of the column that leads to reduction of the Euler buckling stress. Sectional area is descript as:

A_w is the sectional area of stiffener
A_T is the sectional area of a single longitudinal stiffener plus effective plating

The buckling coefficient is obtained the same way as for a panel with small stiffeners and as before takes into account the panel geometric properties.

2.4 Steel sandwich plate (SSP)

2.4.1 General introduction

The steel sandwich structure (SSP it is a composite structure with different stretching abilitys in different directions whichoffer substantial advantages in design because of its enormous ability to absorb and distribute energy. Its structure has for a long time been used in industries like ship, air planes and recently increased popularity in bridge design. It's high strength to weigh ratio and energy absorption is a great combination when facing high winds, storm, earthquakes and accidental impact loads, to name a few(Poirier, Vel, & Caccese, 2013). Its greatest problem so far has been the production, because of a lack in laser technology the process was slow and not effective enough. With great enhancements in that field of laser welding and implementation of Hybrid laser welding a great promise of fast production with improved fatigue strength at a reasonable cost, means great promise for the SSP(Abbott, Systems, & Caccese, 2007).

The SSP is always a combination of two stiff face sheets and a less stiff core configuration but a lot of different core configurations exist and they all have different application fields. A great rule of thumb is that the core should weight the same as the plat sheets in order to have good structural performance. In Figure 2.7 a number of common core figurations are shown and below their main abilities. (Alwan & Järve, 2012).

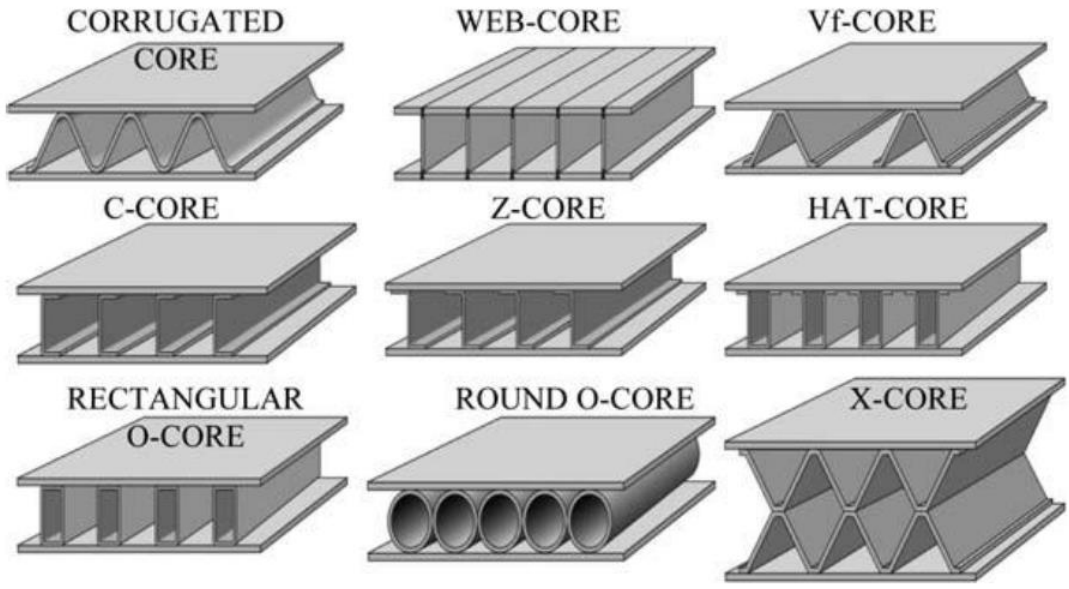

Figure 2.7. Different SSP core figurations (Romanoff & Versa 2006).

- X-core has great energy absorption.
- O-core has high nominal stiffness.
- Z- and C-core have high bending and shear stiffness in the direction of the core.
- Corrugated-core has a superior overall stiffness in both directions compared to other configurations.

2.4.2 Mindlin-Reissner and Kirchoff plate theory

Plate theory was discussed in the first chapter for the general simple plate case where Euler's theory played a large role. Two main plate theories will be discussed that have been developed for representing 3D structures as equivalent 2D plates. They are firstly the addition to Euler-Bernoulli, Kirchoff theory and then the extension to Kirchoff, Mindlin-Reissner plate theory. The first basic difference between the two is that Kirchoff theory applies for thin plates whereas Mindlin-Reissner is meant for thick plates. Mindlin-Reissner assumes that the normal remains straight but not necessarily normal to the neutral plate. (Tan, Montague, & Norris, 1989). In Kirchhoff theory it is assumed that normal remains straight and orthogonal to the middle plane after deforming. This means that no transverse shear deformation is accounted for it the Kirchoff theory. In the case of SSP, this means that Kirchoff theory is not a viable option because transverse shear deformation is too large of an effect to be neglected. Therefor the Mindlin-Reissner is preferable in the case of SSP because it gives a more accurate approximation of the behaviour of these thick, shear flexible plates.

2.4.3 Stiffness parameters

In 1948 Libove and Batdarf developed the Small deflection theory which was a way of idealizing the 3D structure of a sandwich plate as a homogeneous orthotropic 2D plate. The 2D plate referred to as an equivalent 2D plate was idealized with the use of stiffness parameters that describe the behaviour of the 3D structure (Libove & Batdorf, 1948). These constants where:

- E_x Axial stiffness in x-direction
- E_y Axial stiffness in y-direction
- D_x bending stiffness in x-direction
- D_y bending stiffness in y-direction
- D_{xy} twisting stiffness
- D_{Qx} transverse shear stiffness
- D_{Qy} transverse shear stiffness
- G_{xy} horizontal shear stiffness

As well needed are the two Poisson's ratios:

- ν_x Poisson's ratios in x-direction
- ν_y Poisson's ratios in y-direction

Later on in 1951 Libove and Hubka derived equations and investigated the stiffness parameters for the case of corrugated-core sandwich plates. In their research they made the assumption that "straight lines normal to the middle surface were assumed to remain straight, but not necessarily normal to the middle surface during distortion of the plate"(Libove & Hubka, 1951).

In 2005 a paper was published by Cheng where they prompt a numerical approach to evaluate the stiffness parameters $D_x, D_y, D_{xy}, D_{Qx}\ and\ D_{Qy}$ (Chang et al., 2005). In their research they compare 3D corrugated core sandwich to 2D homogeneous, thick, orthotropic plate. Their assumptions are similar to the ones (Libove & Hubka, 1951) made. They compared their results to both analytical and 3D modelling made by (Tan et al., 1989). The result they got was quite accurate compared to previous analytical and experimental work.

In 2014 Beneus and Koc analysed steel sandwich panels with a corrugated-core and made a Mathcad routine where they numerically derived the stiffness parameters and the deflection for out of plane loading. These stiffness parameters where based on the expressions Libove and Hubka derived in 1951. They made the optimisation process in the way so the individual parts of the section would not exceed cross-sectional class three in order to exclude local buckling within a given limit(Beneus & Koc, 2014).

In 2015 alongside this current master thesis (Dackman & Ek, 2015) utilized the Mathcad routine Beneus and Koc did in 2014. While going through the derivations and comparing them to Libove and Hubka stiffnesses they discovered an error in the derivation of the transvers shear stiffness factor D_{Qy} which they fixed. This improved Mathcad routine was utilized in this present work to derive the stiffness factors as well as using its deflection routine to compare with the FEM 2D equivalent model.

2.4.4 Elastic stiffness constants for SSP

The elastic stiffness constants used in the Mathcad optimisation routine developed by Beneus and Koc in 2014 were derived by Libove and Hubka in 1951 see the stiffnesses in Figure 2.8. The Mathcad routine was then enhanced by David and Walter in 2015 by including the option of having different thickness of the top flange and bottom flange of the SSP. The equations for the stiffness parameters used in the Mathcad routine will now be explained.

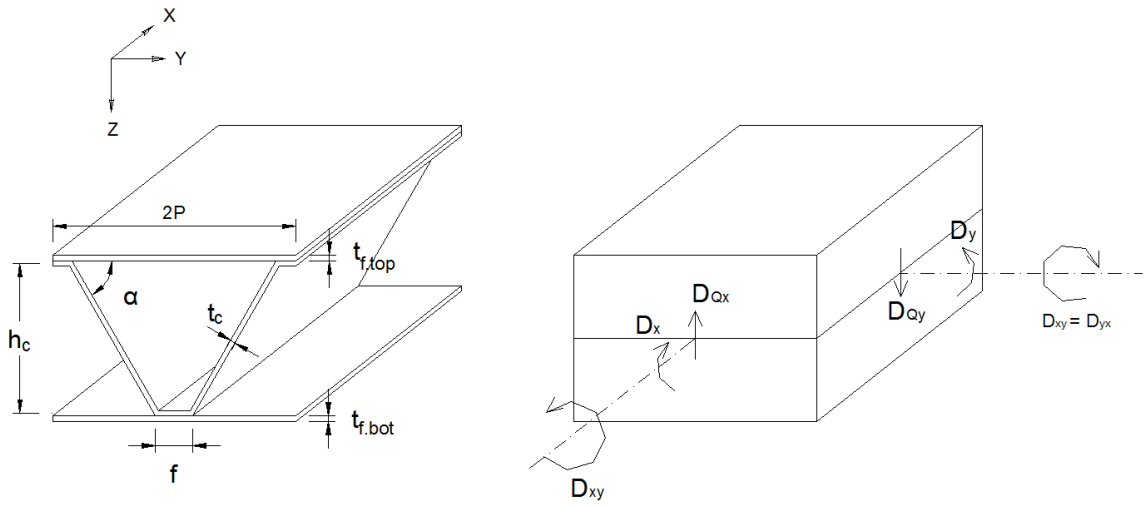

Figure 2.8. Corrugated-core 3D sandwich plate and the idealized 2D equivalent plate, including all parameters.

- **E_x *and* E_y -Axial stiffness per unit meter [N/m]**

$$E_x = E_f A_f + E_c A_c \qquad (2.25)$$

$$E_y = \frac{E_f A_f}{1 - \nu_f^2 \left(1 - \frac{E_f A_f}{E_x}\right)} \qquad (2.26)$$

Where:

A_f	$t_{f.top}$ plus $t_{f.bot}$
E_c	modulus of elasticity core material
E_f	modulus of elasticity of face sheet
$t_{f.top}$	thickness of the top face sheet
$t_{f.bot}$	thickness of the bottom face sheet
A_c	area of the web per meter
ν_f	Poisson's ratio of the face sheet material

The Poisson's ratios associated with extension are given in equations:

$$\nu_x' = \nu_f \qquad (2.27)$$

$$\nu_y' = \nu_x' \frac{E_y}{E_x} \qquad (2.28)$$

- **D_x *and* D_y** -Bending stiffness per unit meter [Nm]:

$$D_x = E_f I_f + E_c I_c \qquad (2.29)$$

$$D_y = \frac{E_f I_f}{1 - \nu_f^2 \left(1 - \frac{E_f I_f}{D_x}\right)} \qquad (2.30)$$

Where:

I_f Moment of inertia, per unit width, of face sheets cross-sectional area taken around the central axis

I_c Moment of inertia, per unit width, of corrugated cross-sectional area taken around the central axis,

ν_f Poisson's ratio of face sheet material

The Poisson's ratios associated with bending are given in equations:

$$\nu_x = \nu_f \qquad (2.31)$$

$$\nu_y = \nu_x \frac{D_y}{D_x} \qquad (2.32)$$

- $\boldsymbol{D_{xy}}$ -Torsional stiffness per unit meter [Nm]

$$D_{xy} = 2\left[G_f t_{f.top} k_{GJ}^2 + \frac{G_c t_c}{A_c}\left(k_{GJ} - k_c\right)^2 + G_f t_{f.top}\left(1 - k_{GJ}\right)^2\right] h^2 \qquad (2.33)$$

Where:

G_f Shear modulus of elasticity of face sheet material

G_c Shear modulus of elasticity of core material

t_c Thickness of corrugated core sheet

k_{GJ} Ratio depending on the distance to the zero-shear plane

k_c Ratio depending on the distance to the shear centre of the corrugation

- $\boldsymbol{G_{xy}}$ -Horizontal shear stiffness per unit meter [N/m]

$$G_{xy} = \frac{G_c t_c^2}{A_c} + G_f A_f \qquad (2.34)$$

- $\boldsymbol{D_{Qx}}$ ***and*** $\boldsymbol{D_{Qy}}$ -Transverse shear stiffness per unit meter [N/m]

$$D_{Qx} = \frac{G_c I t_c h}{p \int_0^{l_c} Q ds} \qquad (2.35)$$

Where:

Q	Static moment of hatched area about the neutral axis
I	Moment of inertia of cross section of width $2p$ about central axis
h	Distance between middle surfaces of face sheets
p	Half of the corrugation pitch
l_c	Length of one corrugation leg, measured along the centre line

In figure 2.9 the constants are further explained.

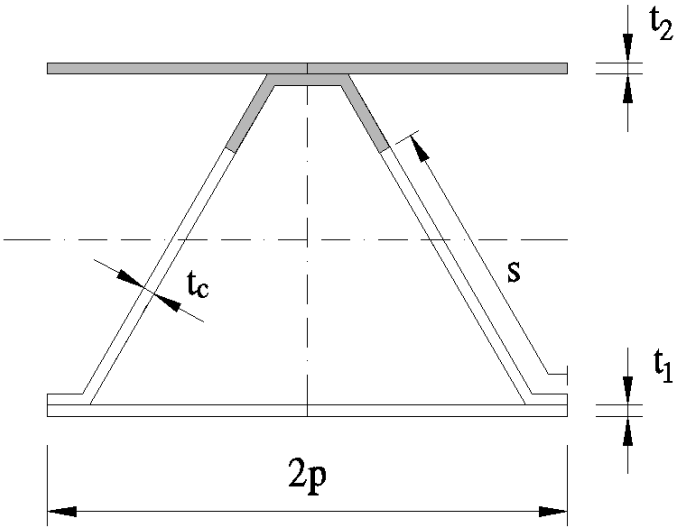

Figure 2.9. Area to be used when calculating the static moment of area.

By assuming that the face sheets carry the entire bending and none is carried by the web equation (2.35) can be simplified into equation (2.36)

$$D_{Qx} \approx \frac{G_c t_c^2}{A_c} \left(\frac{h}{p}\right)^2 \qquad (2.36)$$

$$D_{Qy} = Sh \left(\frac{E_c}{1 - \nu_c^2}\right) \left(\frac{t_c}{h_c}\right)^3 \qquad (2.37)$$

Where:

h_c Depth of corrugation, measured vertically from centre line of crest to centre line at trough, [m]

ν_c Poisson's ratio of core material, [-]

S Non-dimensional coefficient depending upon shape of corrugation, relative proportions of sandwich cross section, and the material properties of the component parts, [-]

2.4.5 General shell stiffness

The general shell stiffness model in a good model to use when both out-of-plane loading and in-plane loading needs to considered in the analysis. Since in the analysis made in this master thesis both loading cases are used as well as the main analysis being buckling the general shell stiffness model was chosen instead of the lamina model which only works with either in-plane loading or out-of-plane loading at once. General shell section response is described with Equation (2.38).

$$\{N\} = [D]\{E\} \qquad (2.38)$$

Where:

$\{N\}$ Membrane forces and bending moments per unit length on the shell section

$[D]$ Section stiffness matrix

$\{E\}$ Generalised section strains in the shell

Equation (2.38) can be written in the following form where the stiffness terms are given below:

$$\begin{Bmatrix} N_{11} \\ N_{22} \\ N_{12} \\ M_{11} \\ M_{22} \\ M_{12} \end{Bmatrix} = \begin{bmatrix} D_{11} & D_{12} & 0 & 0 & 0 & 0 \\ D_{21} & D_{22} & 0 & 0 & 0 & 0 \\ 0 & 0 & D_{33} & 0 & 0 & 0 \\ 0 & 0 & 0 & D_{44} & D_{45} & 0 \\ 0 & 0 & 0 & D_{54} & D_{55} & 0 \\ 0 & 0 & 0 & 0 & 0 & D_{66} \end{bmatrix} \begin{Bmatrix} \varepsilon_{11} \\ \varepsilon_{22} \\ \gamma_{12} \\ \kappa_{11} \\ \kappa_{22} \\ \kappa_{12} \end{Bmatrix}$$

Where the stiffness factors are:

$$D_{11} = \frac{E_x}{1 - \nu_x' \nu_y'} \qquad (2.39)$$

$$D_{12} = D_{21} = \frac{\nu_x' E_y}{1 - \nu_x' \nu_y'} = \frac{\nu_y' E_x}{1 - \nu_x' \nu_y'} \qquad (2.40)$$

$$D_{22} = \frac{E_y}{1 - \nu_x' \nu_y'} \quad (2.41)$$

$$D_{33} = G_{xy} \quad (2.42)$$

$$D_{44} = \frac{D_x}{1 - \nu_x \nu_y} \quad (2.43)$$

$$D_{45} = D_{54} = \frac{\nu_x D_y}{1 - \nu_x \nu_y} = \frac{\nu_y D_x}{1 - \nu_x \nu_y} \quad (2.44)$$

$$D_{55} = \frac{D_y}{1 - \nu_x \nu_y} \quad (2.45)$$

$$D_{66} = \frac{1}{2} D_{xy} \quad (2.46)$$

Where the Poisson´s ratios are:

$$\nu_y' = \nu_x' \frac{E_y}{E_x} \quad (2.47)$$

$$\nu_y = \nu_x \frac{D_y}{D_x} \quad (2.48)$$

How the stiffnesses are utilized in the general shell stiffness model in ABAQUS can be seen in Figure 2.10 and Figure 2.11. In the stiffness part the K-matrix is filled in with the stiffness factors derive in equations (2.39) – (2.46). In the advanced part the shear stiffnesses are inserted directly from the derivations from chapter 2.4.4. Where the k factors are:

- K_{11} - Value of the shear stiffness of the section in the first direction.
- K_{22} - Value of the shear stiffness of the section in the second direction.
- K_{12} - Value of the coupling term in the shear stiffness of the section.

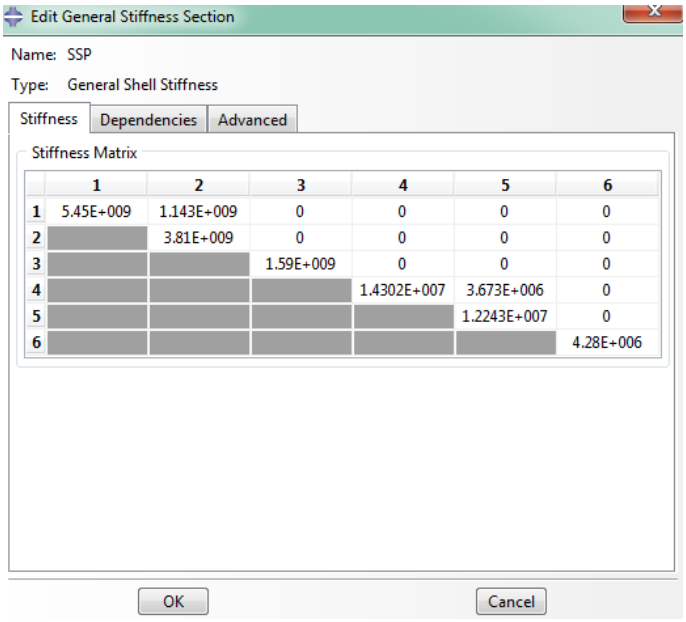

Figure 2.10. Stiffness factors entered into the k-matrix in the general shell stiffness in ABAQUS.

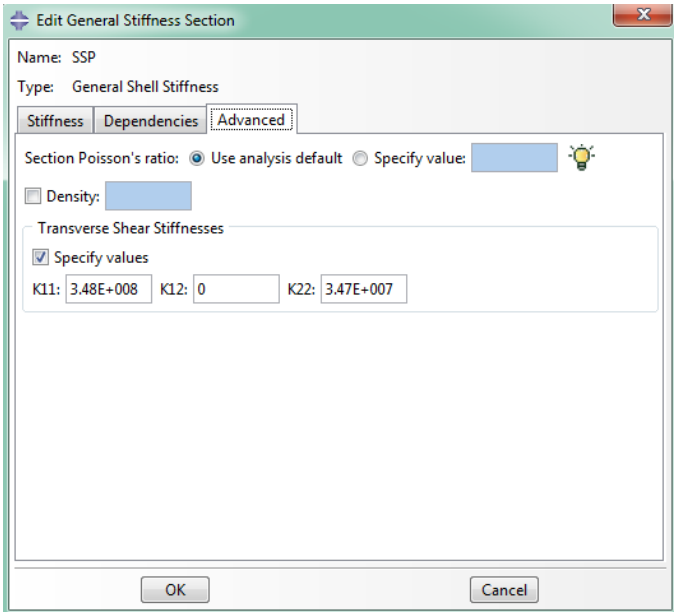

Figure 2.11. Transverse shear stiffness's entered in the general shell stiffness in ABAQUS.

2.4.6 Source of error in modelling

Between the 3D and 2D models there are causes of error that can be pointed at as a likely reason for the differences between the two. The first being the obvious geometrical differences where on the one hand a full size 3D model can have interaction problems between elements and local buckles. On the other hand the 2D model can never experience these kind of localized problems because it is only a simple plate.

Two sources of error can be directly traced to how the 3D model was modelled:

1. All of the SSP section was modelled using shell elements including the connection between the flanges and the web, the weld. When ABAQUS gives these shell element thickness the intersections do not connect perfectly, see Figure 2.12. This will cause some of the web to overlaps and a gap forms as well causing a small decrease in stiffness.
2. The weld between the web and the flange gets the same thickness as the web which increases the stiffness somewhat of the 3D model.
3. In the parametric study the same cross-section modelled in ABAQUS is used but the flanges and web thickness is increased. This will cause some part of the web and the flange to overlap in the 3D model which would not happen in the 2D model.

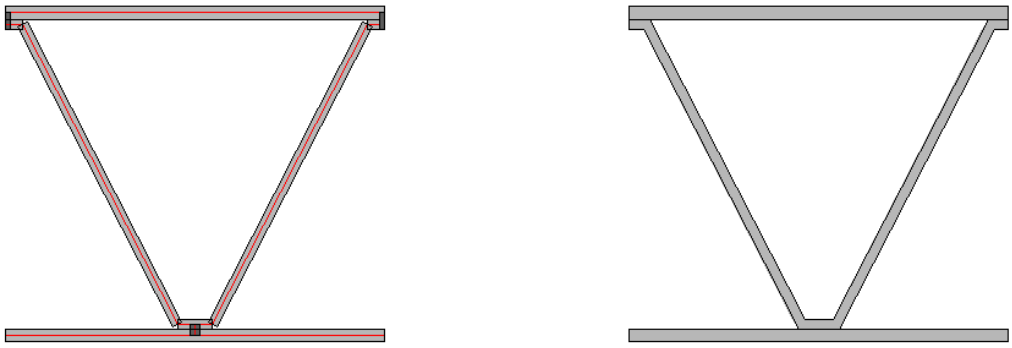

Figure 2.12. SSP cross-section on the left is how it acts in ABAQUS, of the right how it acts is in reality.

A study was made to quantify the volume of error which the incaution of the welds in the 3D model had by calculating the stiffness of the weld and adding them to bending stiffness D_x. Panel C1 from section 5.4 was used to compare the critical buckling stress. The original 3D results with the weld included gave the critical buckling stress of 315 [MPa] while the original 2D equivalent model which did not include the welds gave the critical buckling stress of 289 [MPa] which is quite some difference and some of this difference could be explained with this added stiffness from the welds. The stiffness of the welds was calculated and added to into the 2D equivalent model and that gave a critical buckling stress of 294 [MPa] which is an increase of 5 [MPa] see table 2.1.

Table 2.1. Effect of taking weld into consideration while modelling in 3D and 2D.

Panel nr.	Size [m]	Model	Weld	σ_{ref} [MPa]	λ_{ref}	σ_{cr} [MPa]
C1	*6x18*	*3D FEM*	*with weld*	*325*	*0,97026*	*315*
C1	*6x18*	*2D FEM*	*With o. weld*	*325*	*0,88941*	*289*
C1	*6x18*	*2D FEM*	*with weld*	*325*	*0,90373*	*294*

2.4.7 Approximate analytical solution for simply supported, orthotropic SSP with thin faces

The approximate analytical solution for an orthotropic sandwich plate for a various edge conditions is given in (Zenkert, 1995) chapter 9.8 where energy relation is used to derive the buckling load for SSP. For a plate with simply supported boundaries and a uniaxial buckling (P_x = P and P_y =0) where the minimum buckling load is only a one wave length in y-direction (n=1) the plate deflection can be obtained from:

$$w = w_b + w_S = (\overline{w_b} + \overline{w_s}) \sin\left(\frac{m\pi x}{a}\right) \sin\left(\frac{n\pi y}{b}\right) \qquad (2.49)$$

Where:

- a length of the plate
- b width of the plate
- m number of buckling waves in x-direction
- n number of buckling waves in y-direction

Another equation obtained from (Zenkert, 1995) chapter 8.8 gives the approximation for the total energy in terms of partial deflection:

$$U_{se} = \frac{1}{2}\int\int\left[\frac{D_x}{1-\nu_{xy}\nu_{yx}}\left(\frac{\partial^2 w_b}{\partial x^2}\right)^2 + \frac{\nu_{yx}D_x + \nu_{xy}D_y}{1-\nu_{xy}\nu_{yx}}\left(\frac{\partial^2 w_b}{\partial x^2}\right)\left(\frac{\partial^2 w_b}{\partial y^2}\right) + \frac{D_y}{1-\nu_{xy}\nu_{yx}}\left(\frac{\partial^2 w_b}{\partial y^2}\right)^2 + 2D_{xy}\left(\frac{\partial^2 w_b}{\partial x \partial y}\right)^2 + S_x\left(\frac{\partial w_s}{\partial_x}\right)^2 + S_y\left(\frac{\partial w_s}{\partial_y}\right)^2\right] dxdy \qquad (2.50)$$

Inserting equation (2.49) into equation (2.50) yields:

$$U = \frac{\overline{w_b}^2\pi^4}{2}\left[\frac{D_x m^4 b}{4a^3\left(1-\nu_{xy}\nu_{yx}\right)} + \frac{D_y a}{4b^3\left(1-\nu_{xy}\nu_{yx}\right)} + \frac{\nu_{xy}D_x m^2}{2ab\left(1-\nu_{xy}\nu_{yx}\right)} + \frac{D_{xy}m^2}{2ab}\right] + \frac{\overline{w_s}^2\pi^2}{2}\left[\frac{S_x m^2 b}{4a} + \frac{S_y a}{4b}\right] - \frac{P(\overline{w_b}+\overline{w_s})^2 m^2\pi^2 b}{8a} \quad (2.51)$$

Equation (2.51) gives the total potential energy for the plate and from the same equation two different ways can be used to determining the buckling load P. The most accurate way is to state that the buckling load can be found when total potential energy U for the plate is lowest. This estimation can be difficult so another much simpler approach which has be shown to yield the same results can be used. The method calculates the total load needed for the SSP to buckle where the buckling load for pure bending and buckling load for pure compression are calculated separately and then added together to find the total buckling load. The total buckling load can be obtained from:

$$\frac{1}{P} = \frac{1}{P_b} + \frac{1}{P_s}\ , with\ w = w_b + w_s \quad (2.52)$$

Where:

P total buckling load
P_b buckling load due to bending
P_s buckling load due to shear

The buckling load in pure compression is then found by:

$$\left[\frac{\partial U}{\partial \overline{w}_b}\right]_{w_s=0} \quad (2.53)$$

That gives:

$$\frac{1}{P_b} = \frac{b^2\left(1-\nu_{xy}\nu_{yx}\right)}{\pi^2\left(D_x\left(\frac{mb}{a}\right)^2 + D_y\left(\frac{a}{mb}\right)^2 + 2\left(\nu_{xy}D_x + D_{xy}\left(1-\nu_{xy}\nu_{yx}\right)\right)\right)} \quad (2.54)$$

Where:

D_x bending stiffness in x-direction
D_y Bending stiffness in y-direction
D_{xy} twisting stiffness
ν_x poisson's rations

ν_x poisson's rations

The buckling load in pure shear is then found by:

$$\left[\frac{\partial U}{\partial \bar{w}_s}\right]_{w_s=0} \qquad (2.55)$$

That gives:

$$\frac{1}{P_s} = \frac{1}{S_x + S_y\left(\frac{a}{mb}\right)^2} \qquad (2.56)$$

Where:

S_x Shear stiffness x-direction
S_y Shear stiffness y-direction

Now when the total buckling load P has been calculated the critical buckling stress can be found by divide the total buckling load into the plate area per meter.

$$\sigma_{cr} = \frac{P}{A} \qquad (2.57)$$

3 EBPlate

3.1 Introduction

A software called Elastic Buckling of Plate (EBPlate) was designed and develop by the "Centre Technique Industrial de la Construction Métallique" with a partial funding from European Research Fund for Coal and Steel to help with calculation of critical buckling stress of panels. EBPlate is designed to calculated critical buckling strength of rectangular plate with or without stiffeners subjected to in-plane load. Stiffeners can be assigned to the plate as longitudinal and/or transverse stiffeners of which EBPlate offers a number of different options. EBPlate gives also the possibility to calculate critical buckling stress for an orthotropic plate for any given geometry by smearing equally spaced stiffeners over the panel.

Due to lack of analytical formulae in Annex A of EN 1993-1-5 and also that the formulas neglect some favourable effects for a stiffened panels this software has been designed to help users to estimate critical buckling stress for a panel when it comes to design. Designer has been provided with practical tools to calculate with more accuracy the value of elastic critical buckling stresses in plates without neglected favourable effects (e.g. torsional stiffness of stiffeners and rotational restraint at edges) and also avoiding time consuming finite element modelling .(Galéa & Martin, 2010)

3.2 General methodology for calculation of elastic critical buckling stress

Calculation of elastic critical buckling stress for a plate are carried out in EBPlate based on the minimum factor φ_{cr} and the reference stresses (σ_x, σ_x, τ). For a reference stress defined by user the critical stresses can be obtained from:

$$\sigma_{x.cr} = \phi_{cr}\, \sigma_x \qquad (3.1)$$

$$\sigma_{y.cr} = \phi_{cr}\, \sigma_y \qquad (3.2)$$

$$\tau_{cr} = \phi_{cr}\, \tau \qquad (3.3)$$

The minimum factor φ_{cr} is calculated based on the Rayleigh-Ritz method (energy method) and is expressed by a Fourier series:

$$w(x,y) = \sum_{m=1}^{m_{max}} \sum_{n=1}^{n_{max}} \left(a_{mn} \sin\left(\frac{m\pi x}{a}\right) \sin\left(\frac{n\pi y}{b}\right)\right) \qquad (3.4)$$

Where:

m_{max}	maximum number of half-waves considered in the x-direction
n_{max}	maximum number of half-waves considered in the y-direction
a_{mn}	displacement parameters or degrees of freedom of the system

Variations of energy can be described and at instability it can be expressed as:

$$\Delta U - \Delta W_{int}(S_{cr}) = 0 \qquad (3.5)$$

Where:

ΔU	variation of strain energy of the plate
$\Delta W_{int}(S_{cr})$	variation of internal work of critical stresses S_{cr}
$S_{cr} = \phi_{cr} S$	critical stresses

Then the following eigenvalue problem can be solved for the lowest eigenvalue ϕ_{cr} :

$$\det[R_0 - \phi_{cr} R_G(S)] = 0 \qquad (3.6)$$

Where:

R_0	Initial stiffness matrix (from strain energy)
R_G	Geometrical stiffness matrix (from internal work of stresses)

For calculation of element at line i and column j for each matrix is obtained from:

$$r_{ij} = \frac{\partial^2(\Delta U)}{\partial a_i \partial a_j} \; for \; R_o \qquad (3.7)$$

$$r_{ij} = \frac{\partial^2(\Delta W_{int}(S))}{\partial a_i \partial a_j} \; for \; R_o \qquad (3.8)$$

The total strain energy can be expressed like:

$$\Delta U = \Delta U_p + \Delta U_{sx} + \Delta U_{sy} + \Delta U_{er} \qquad (3.9)$$

Where:

ΔU_p	Strain energy of the plate itself
ΔU_{sx}	Strain energy of longitudinal stiffeners
ΔU_{sy}	Strain energy of transverse stiffeners
ΔU_{er}	Strain energy of edge rotational restraints

Total initial work can be expressed like:

$$\Delta W_{int} = \Delta W_p + \Delta W_{sx} + \Delta W_{sy} \qquad (3.10)$$

Where:

ΔW_p Internal work of stresses of the plate itself
ΔW_{sx} Internal work of normal forces in longitudinal stiffeners
ΔW_{sy} Internal work of normal forces in transverse stiffeners

3.3 Calculation

3.3.1 Stiffener's Characteristics

When it comes to stiffened plates, stiffeners are assigned to a panel either as longitudinal stiffeners or transvers stiffeners. The software offers a number of predefined type of stiffeners section that are defined by the dimension of the stiffener. From this predefined section the characteristics for each stiffener can be established:

$$\delta = \frac{A_s}{b \cdot t} \qquad (3.11)$$

$$\theta = \frac{G \cdot J_s}{b \cdot D} \qquad (3.12)$$

$$\gamma = \frac{E \cdot I_s}{b \cdot D} \qquad (3.13)$$

Where:

δ relative axial stiffness
A_s area of the section (effective width plus the stiffener)
b width of the whole plate
t thickness of the plate
θ relative torsional stiffness
G shear modulus
J_s torsional inertia of the section
D flexural stiffness of the plate
γ flexural stiffness of stiffener
E elastic modulus
I_s flexural inertia of the section

It is also possible to calculate the characteristics for any section without using the predefined section and use the value in EBPlate. It should be noted that the flexural inertia is calculated about the natural axis and takes into account the stiffeners and also the effective with of the plate. Effective with of the plate is defined by the factor k times the thickness of the plate where k=10. Examples of effective plate are showed in Figure 3.1.

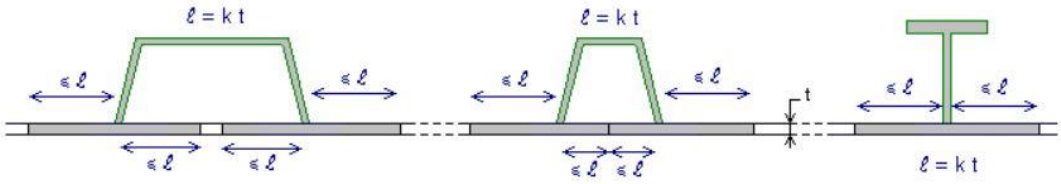

Figure 3.1. How effective width is estimated in EBPlate.

Bear in mind that use of EBPlate to calculate critical buckling stress is only recommended if a minimum stiffener rigidity is higher than 25 ($\gamma > 25$). Values that are lower than 25 can give higher value for the characteristic resistance of the stiffeners and therefore give unreasonable results (Galéa & Martin, 2010).

3.3.2 Global buckling and local buckling

When it comes to calculation of critical buckling stress for a panel without stiffeners or panel with stiffeners two different types of buckling should be consider, global buckling and local buckling. EBPlate is deigned to calculate the first buckling mode without considering the type of buckling (local buckling or global buckling) by taking into account separately or simultaneously the presence of discrete stiffeners and orthotropic behaviour of plates.
For a stiffened plate under axial load the changes in stress of the plate can be described as in Figure 3.2. The plate will have global buckling until the relativity flexural stiffness of the stiffeners is $\gamma=\gamma^*$, after that the stiffeners hinder global buckling and divides the plate into smaller areas resulting in local buckling.

A

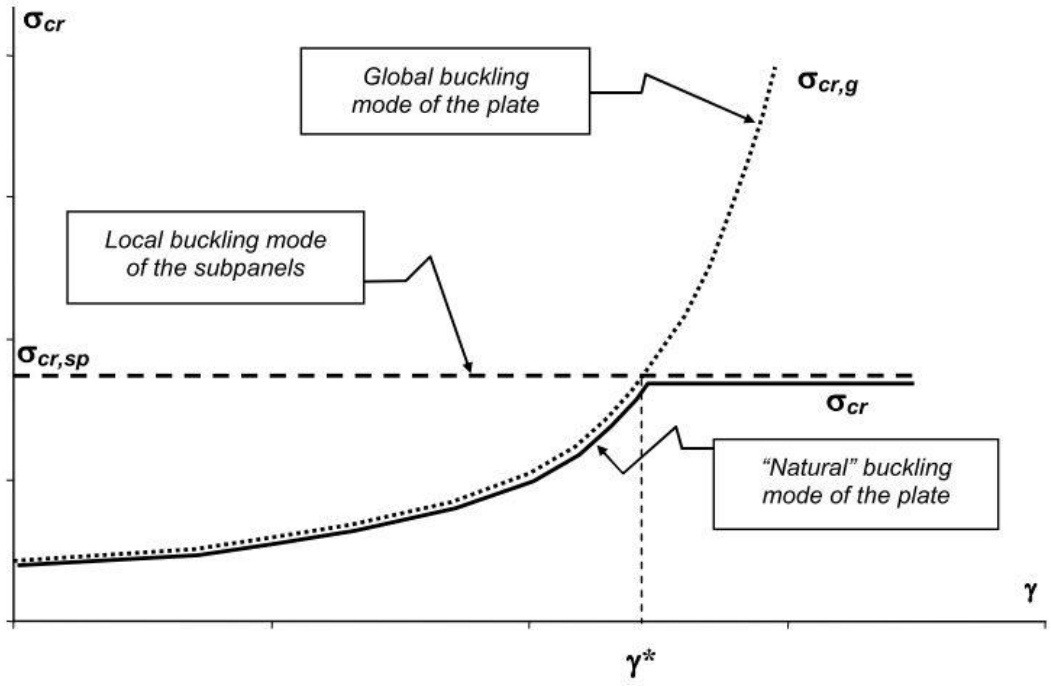

Figure 3.2. Buckling mode of the stiffened plate and associated critical buckling stresses

EBPlate offers the possibility to show only global buckling of a plate and neglect all local buckling. This can be accomplished by making the assumption that there are no stresses in the stiffened panel itself and all stress are taken by the stiffeners and the effective width of the plate. This can be achieved by setting the parameter for orthotropic behaviour to minus one (η_x=-1) while all other orthotropic parameters are zero. Than a new modified axial stiffness (δ') of the stiffeners is calculated given by following relations:

$$if \quad \psi_b \geq 0 \quad \delta' = \delta + \left(\frac{3-\psi_t}{5-\psi_b}\frac{b_t}{b} + \frac{2}{5-\psi_b}\frac{b_b}{b}\right) \tag{3.14}$$

$$if \quad \psi_b < 0 \quad \delta' = \delta + \left(\frac{3-\psi_t}{5-\psi_t}\frac{b_t}{b} + \frac{0{,}4}{5-\psi_b}\frac{b_b}{b}\right) \tag{3.15}$$

$$\psi_t = \frac{\sigma_s}{\sigma_t} \tag{3.16}$$

$$\psi_b = \frac{\sigma_b}{\sigma_s} \tag{3.17}$$

The variables (ψ_t and ψ_b) describe the stress distribution on the end of the plate, they are shown and explained in Figure 3.3. The effective width l_t and l_b can be calculated with formulas described in the Annex A of EN 1993-1-5 and are given as:

$$l_t = \frac{3-\psi_t}{5-\psi_t} b_t \tag{3.18}$$

$$if \quad \psi_b \geq 0 \quad l_b = \frac{2}{5-\psi_b} b_b \tag{3.19}$$

$$if \quad \psi_b < 0 \quad l_b = \frac{0{,}4}{5-\psi_b} b_b \tag{3.20}$$

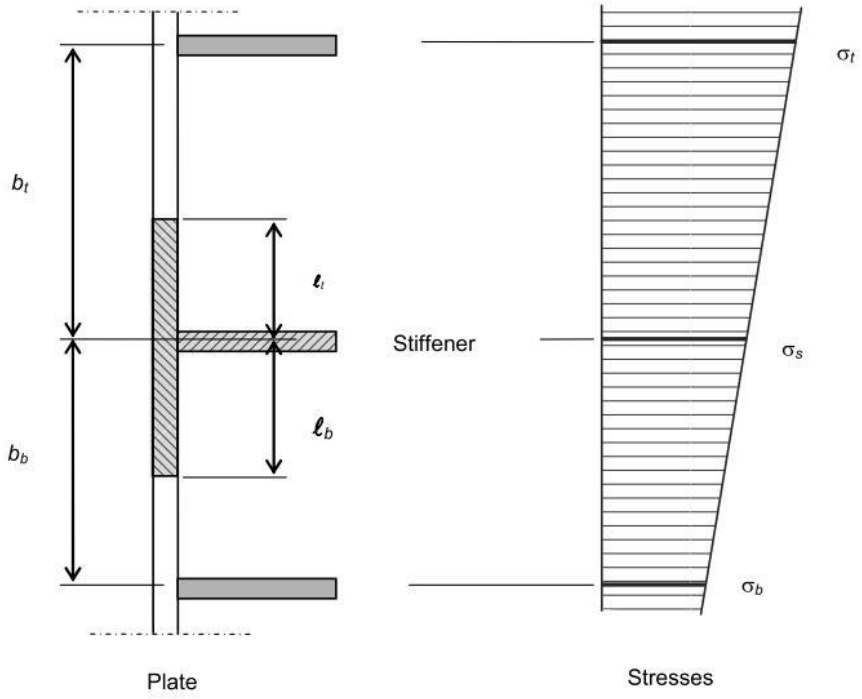

Figure 3.3. Increasing of axial stiffness for a stiffener.

By adding the new modified axial stiffness into EBPlate and change the orthotropic parameter η_x to minus one, EBPlate will give results for the critical buckling stress for global buckling of the plate.

3.3.3 Orthotropic option

EBPlate offers the possibility to estimate the elastic critical buckling stress for a panel by smearing out stiffeners over the panel. EBPlate uses then four coefficients to describe the panel behaviour:

- β_x and β_y that represents the change of transverse flexural plate rigidity, with respect of the reference plate rigidity D.
- η_x and η_y that represent the change of transverse area, with the respect to the reference plate area.

β_x and η_x describe the behaviour for the longitudinal directions of the plate while β_y and η_y describe for the transverse directions. Those parameters can be calculated either by inserting the geometry of the stiffeners and amount into the software or by inserting calculated values for torsional stiffness, flexural stiffness axial stiffness (θ, γ, δ) into the EBPlate as a result of smearing of equally spaced stiffeners.

Another approached is to calculate the orthotropic coefficients and insert directly into the software. The coefficients can be obtained from:

$$\beta_x = \frac{D_x}{D} - 1 \qquad (3.21)$$

$$\beta_y = \frac{D_y}{D} - 1 \qquad (3.22)$$

$$\eta_x = \frac{A_x}{bt} - 1 \qquad (3.23)$$

$$\eta_y = \frac{A_y}{at} - 1 \qquad (3.24)$$

Where:

A_x	area of the section (effective width plus the stiffener)
A_y	area of the stiffened panel
b	width of the whole plate
t	thickness of the plate
D_x	flexural rigidity of orthotropic plate in x-direction
D_y	shear modulus
D	flexural stiffness of the plate

For calculation of critical buckling stress of any plate (stiffened plate or SSP) size of the plate and thickness are required. It is relatively straight forward to find this parameter for a stiffened plate but when it comes to SSP the thickness becomes a problem and has to be estimated. One way for assuming the thickness of the SSP is to find equivalent thickness t_{eq} based on stiffness parameter D_y. It can be assumed that the flexural rigidity stiffness of orthotropic plate with corrugated web is based on the stiffness of the panels (top and bottom panels) shown in Figure 3.4 right, and the corrugated web contributes very little.

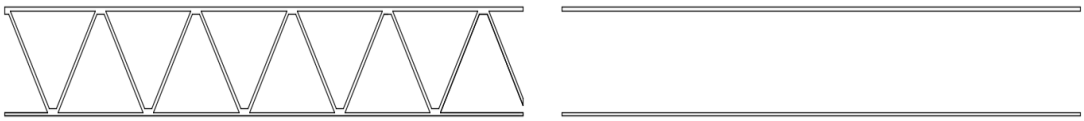

Figure 3.4. How the cross-section is assumed in calculating the rigidity stiffness.

Hence, the assumption is made that the flexural stiffness of the plate is the same as the flexural rigidity stiffness of the orthotropic plate in y-direction and can be written as:

$$D = D_y \qquad (3.25)$$

Flexural stiffness of a plate is defined as:

$$D = \frac{E{t_{eq}}^3}{12(1-\nu^2)} \qquad (3.26)$$

Combining equation (3.25) and (3.28) and solve for t_{eq} the equivalent thickness can be obtained:

$$t_{eq} = \sqrt[3]{\frac{12D(1-\nu^2)}{E}} \qquad (3.27)$$

From equation (3.28) an equivalent thickness for the SSP is established and can be used as the plate thickness in EBPlate.

Hence, in order to utilize EBPlate to estimate the elastic critical buckling stress for an SSP the following variables must be acquired and used as input variables in EBPlate.

- The elastic constants from chapter 2.4.4
- Length and width, a and l respectively, of the plate
- The equivalent thickness of plate given in equation (3.27)

4 Modelling and results for stiffened plates

4.1 Introduction

In this chapter a parametric study is conducted on four stiffened plates with various number and size of stiffeners which are further discussed in the geometrical section. The panels were chosen to test both plate-like behaviour and the column-like behaviour. Most of the chapter covers the finite element analysis done in ABAQUS in great detail and in the end the analytical methods, EBPlate and the finite element analysis compared and the results reviewed.

The finite element analysis were an eigenvalue buckling analysis by modelling the stiffened plates as 3D structures using shell elements. For verification of modelling technique, first a one load step static general analysis where run and the stress distribution inspected. The stress distribution had to be evenly distributed with no irregularities in order for the model to be deemed accurate. Once the model had been verified linear elastic buckling analysis where conducted where the eigenvalue for the global buckling mode was extracted. The modelling technique is discussed further in the modelling section.

4.2 Geometry

For the parametric study four different stiffened plate panels where models with the aim of testing both the plate-like behaviour and column-like behaviour. Theses panels all had the same face sheet thickness of 10mm as well as the stiffeners who also had constants thickness of 10mm. The number and height if the stiffeners, however, varied between panels.

Panels A, B and C all had the objective of testing the plate-like behaviour with various number and size of the stiffeners. All these panels had the aspect ratio of 1 in order to analyse the lowest possible elastic critical buckling value. Panel D had the object of testing the column like behaviour and was therefore chosen to be wide and short to minimize the plate like behaviour.

The stiffened plate panels can be described with a handful of variables which are;

a	Length panel parallel to the loading direction
b	Width of the panel perpendicular to the loading direction
t	Face-sheet thickness
h_w	Height of the stiffener
t_w	Thickness of the stiffener

The geometrical constants for all panels A, B, C and D can be found in Table 4.1 as well as they can be seen in Figure 4.1 and Figure 4.2.

Table 4.1 Geometrical constants for panels used in the parametric study conducted on stiffened plates.

Panel no.	Stiff. no.	a [mm]	b [mm]	t [mm]	h_w [mm]	t_w [mm]
A1	*6*	*2000*	*2000*	*10*	*30*	*10*
A2	*6*	*2000*	*2000*	*10*	*50*	*10*
A3	*6*	*2000*	*2000*	*10*	*80*	*10*
A4	*6*	*2000*	*2000*	*10*	*100*	*10*
A4	*6*	*2000*	*2000*	*10*	*125*	*10*
B1	*10*	*2000*	*2000*	*10*	*30*	*10*
B2	*10*	*2000*	*2000*	*10*	*50*	*10*
B3	*10*	*2000*	*2000*	*10*	*80*	*10*
B4	*10*	*2000*	*2000*	*10*	*100*	*10*
B5	*10*	*2000*	*2000*	*10*	*125*	*10*
C1	*15*	*4000*	*4000*	*10*	*30*	*10*
C2	*15*	*4000*	*4000*	*10*	*50*	*10*
C3	*15*	*4000*	*4000*	*10*	*80*	*10*
C4	*15*	*4000*	*4000*	*10*	*100*	*10*
C5	*15*	*4000*	*4000*	*10*	*125*	*10*
D1	*20*	*2000*	*6000*	*10*	*30*	*10*
D2	*20*	*2000*	*6000*	*10*	*50*	*10*
D3	*20*	*2000*	*6000*	*10*	*80*	*10*
D4	*20*	*2000*	*6000*	*10*	*100*	*10*
D5	*20*	*2000*	*6000*	*10*	*125*	*10*

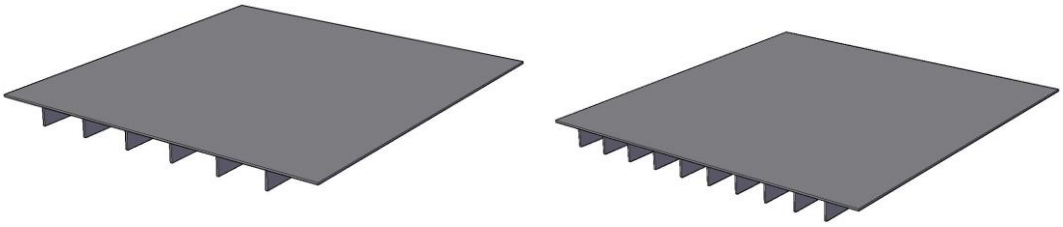

Figure 4.1. Stiffened panels A to left and panels B to right

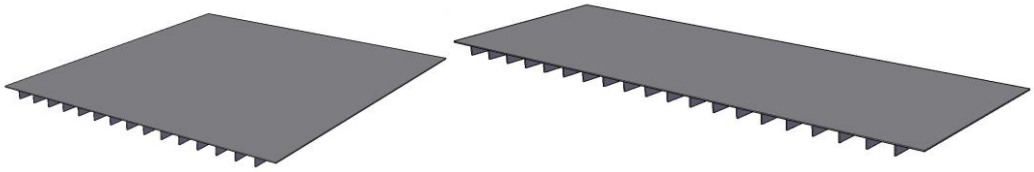

Figure 4.2. Stiffened panels C to left and D to right

4.3 Modelling

All the panels in table 4.1 where modelled in the finite element program ABAQUS as 3D shell elements. First a one load step static analysis was run followed by linear elastic buckling analysis. From the general one load step static analysis the reference critical buckling stress (σ_{ref}) is found. Following the static analysis linear elastic buckling analysis are run and the eigenvalue extracted for the global buckling mode which is in most cases the first buckling mode. This first eigenvalue is the reference eigenvalue (λ_{ref}). Now an estimation of the linear buckling load capacity can be made by multiplying these two reference values see equation 4.1.

$$\sigma_{cr} = \sigma_{ref} \cdot \lambda_{ref} \qquad (4.1)$$

Material

The entire panels is made from steel and the following material properties where assumed and used in the modelling process:

- Material Steel
- Young's modulus 210000 [MPa]
- Poisson's ratio 0,3 [-]

Loading and Boundary conditions

Both edges of the 3D model was loaded with a reference in-plane edge load of 1[N/mm] which corresponded to 0.1 [MPa] of sectional stress. Because in all cases both the face sheet and the stiffeners had the same thickness of 10[mm] it was easy to derive the sectional stress to be 0.1[MPa] in all instances. This sectional stress was then used as the reference stress (σ_{ref}) which multiplied with the reference eigenvalue (λ_{ref}), found in the linear elastic buckling analysis, gives the critical buckling stress (σ_{cr}) see Equation 4.1.

The loading and boundary conditions are explicitly pointed out here below and shown in Figure 4.3:

- Two corner points of the longitudinal (unloaded) edge where fixed in y-direction
- Two corner points of the transvers (loaded) edge where fixed in x-direction
- The longitudinal and transvers edges of the plate are simply supported (fixed in z-direction)
- All the boundary conditions were applied to the face sheet edges
- Shell edge load of 1[N/mm] was applied to the face sheet edge and the stiffeners.

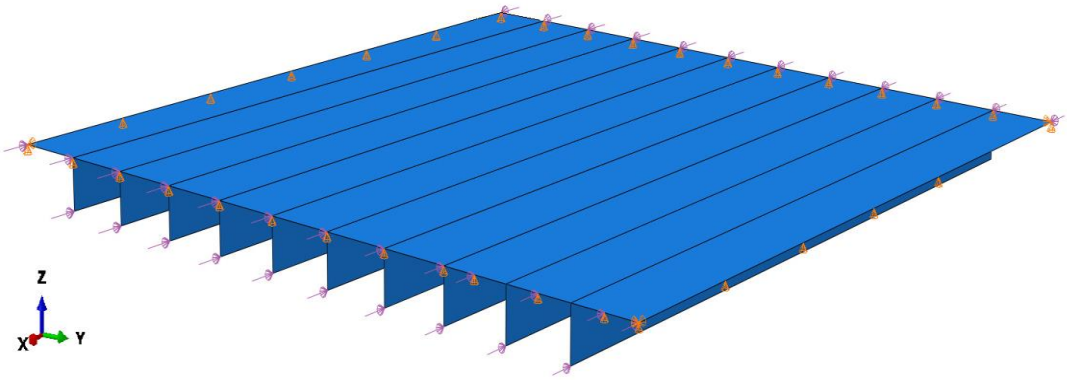

Figure 4.3. 3D shell element model of a stiffened plate showing boundary conditions and loading.

The Static general analysis

The panel was first run in a one load step static general analysis for verifying the stress distribution over the panel. By inspecting the stress distribution in the static analysis it can be verified that the boundary conditions are not effecting the behaviour of the panel and that its behaviour in general is as expected. In all cases the stress distribution was found to be perfect as can be seen in Figure 4.4.

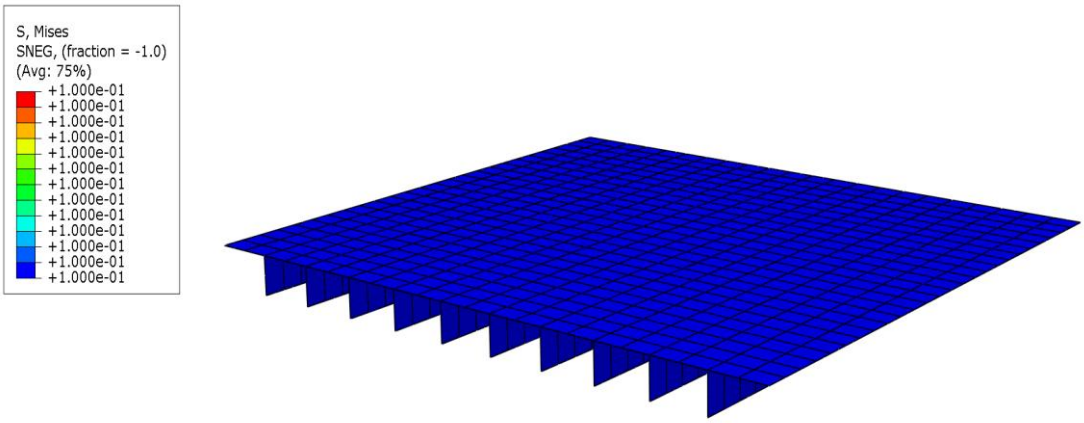

Figure 4.4. Results from a static general analysis of a stiffened plate showing a perfect stress distribution.

Buckling analysis

After the static general analysis and a verification of the stress distribution the analysis was changed to linear elastic buckling analysis. The aim here was to find the global buckling mode and extract the eigenvalue. A result from a successful buckling analysis showing the global buckling made can be seen in Figure 4.5.

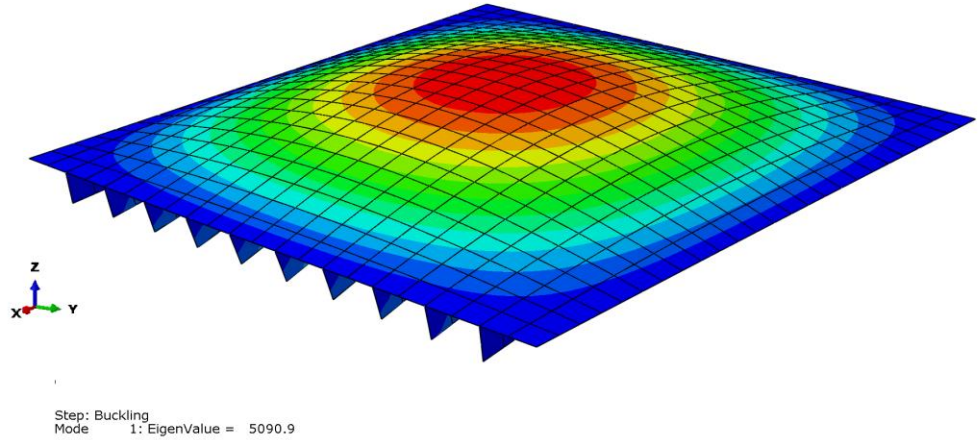

Figure 4.5. Linear elastic buckling results for a stiffened plate showing the global buckling mode.

The result from the linear elastic buckling analysis and the static general analysis was an estimation of the elastic critical buckling stress. A logical next step in the design process would now be to run a none-linear buckling analysis in order to estimate the ultimate load carrying capacity. In the none-linear analyses the initial imperfection, residual stresses and elastic-plastic behaviour of the material, which is the way it is in real life, would be taken into account. But in the aim of this master thesis did not include the ultimate carrying capacity so that was not included in the analysis.

4.4 Convergence study

A conventional convergence study was performed to confirm the result is converging. From the convergence study an estimation of needed elements size for accuracy of the model was be found. The results from the analysis are highly dependent on the internal angle of the mesh, size and the ratio of the sides. The study was performed running the analysis with ever finer grid, from 100 to 30[mm], the difference in between analysis was measured.

The convergence study was made for three different panel size and results are showed in Tables 4.2-4.4. The aim was to have within 10% difference between models as the limit and it is clear from the tables that all samples where well within that limit.

Table 4.2. Results from a convergence study of a 2x2m stiffened plate.

2x2m Panel Mesh size [mm]	σcr [MPa]	Change %
100	*313,24*	-
80	*313,24*	*0,000*
50	*312,92*	*0,102*
30	*312,78*	*0,045*

Table 4.3. Results from a convergence study of a 2x6m stiffened plate.

2x6m Panel Mesh size [mm]	σcr [MPa]	Change %
100	*669,32*	-
80	*668,19*	*0,169*
50	*667,52*	*0,100*
30	*667,07*	*0,067*

Table 4.4. Results from a convergence study of a 4x4m stiffened plate.

4x4m Panel Mesh size [mm]	σcr [MPa]	Change %
100	*1885*	-
80	*1884,6*	*0,021%*
50	*1884,2*	*0,021%*
30	*1884*	*0,011%*

4.5 Results

Different methods have been used for verification of critical buckling stress for a stiffened panels A, B, C and D with numerous stiffeners. Two analytical methods have been used for calculation of critical buckling stress which are discussed in the literature chapter. Numerical calculation have also been used with the help of the software program EBPlate which is discussed in chapter 3. Two different methods where used in EBPlate one where stiffeners are assigned to the plate directly and a second where the plate is converted into an orthotropic plate with assigned stiffness. Finally the most accurate method is the finite element 3D model and all of these methods where compared and the results can be seen in Figures 4.6-9.

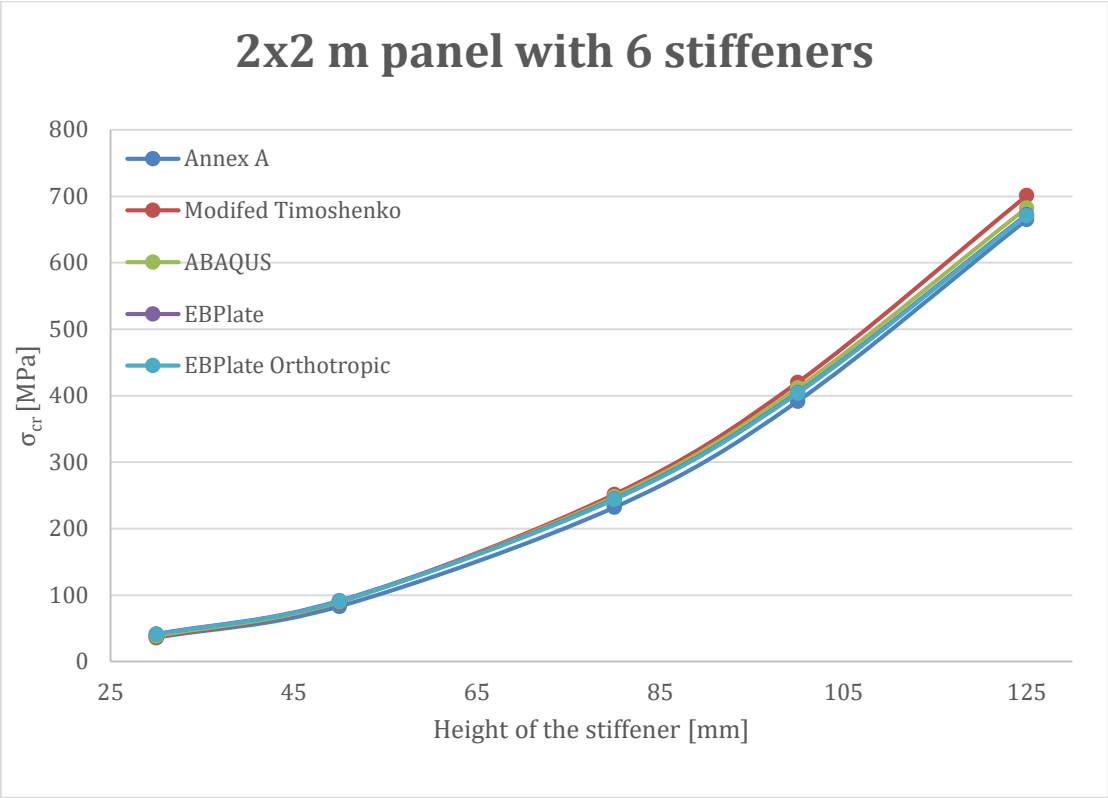

Figure 4.6. Results from all the different methods for stiffened panel A with various stiffener heights.

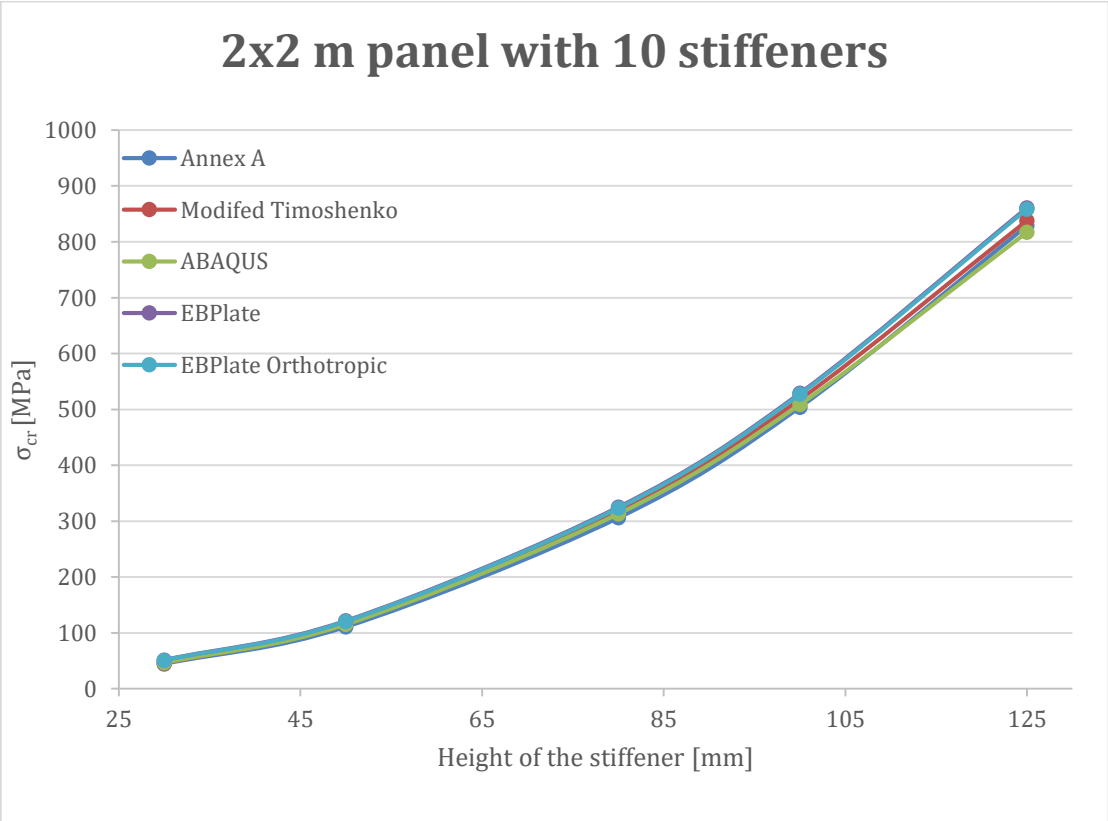

Figure 4.7. Results from all the different methods for stiffened panel B with various stiffener heights.

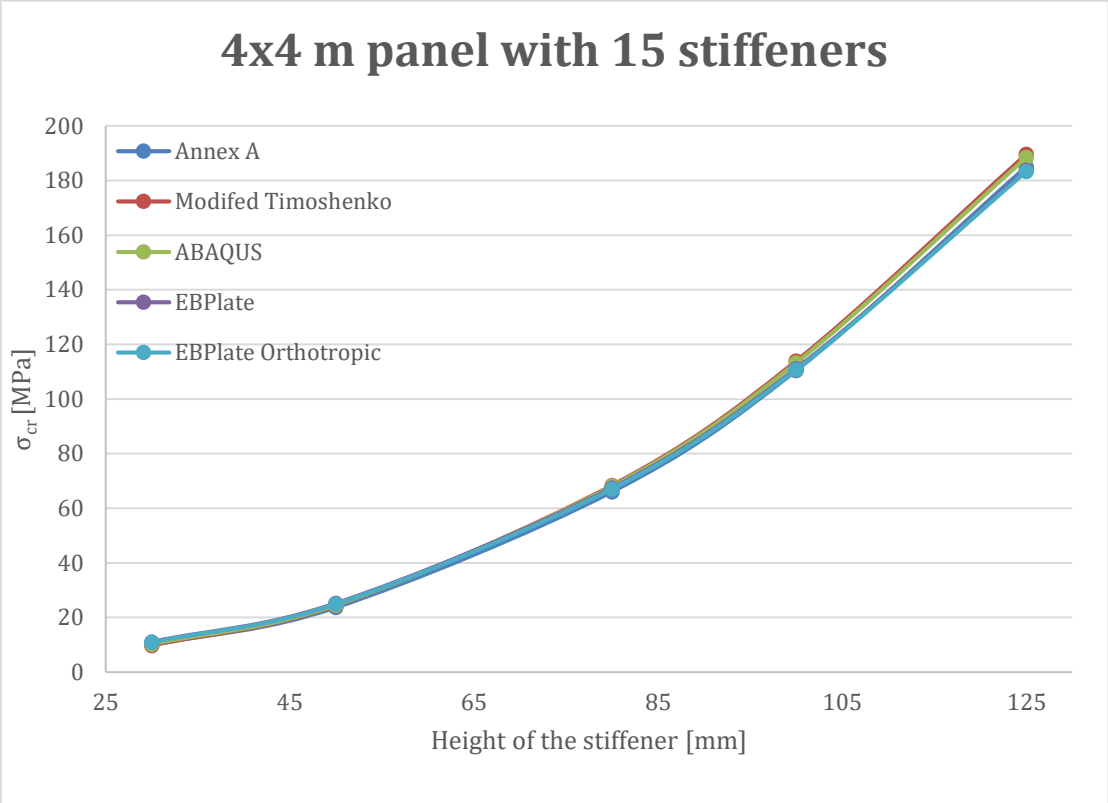

Figure 4.8. Results from all the different methods for stiffened panel C with various stiffener heights.

For all panels the largest difference between models was when the height of the stiffeners was at maximum (125mm). For panel A, Modified Timoshenko had the highest critical buckling stress that was around 5% higher than Annex A which had the lowest critical buckling stress. For panel B, EBPlate orthotropic has the highest critical stress but ABAQUS gives the lowest critical buckling stress, still the difference insignificant, around 5%. Finally, for panel C, the methods are showing similar results and the highest difference is around 3.5%. Modified Timoshenko has the highest while both EBPlate models are showing the same results and have the lowest critical buckling stress.

A small confirmation study was made to see how close to complete column like buckling the models are. The test was carried out for panel number A4 and the value for complete column like buckling was obtained from:

$$\sigma_{cr,col} = \frac{n^2 \cdot \pi^2 \cdot E \cdot I}{A \cdot L^2} = 381{,}2\ [MPa] \qquad (3.28)$$

All the models give higher critical buckling stress than the one calculated by formula 3.28. Annex A gives the highest value of the models, around 405 MPa, and the difference between the calculated column like buckling and the Annex A is approximate 6%. This is reasonable due to the fact that the Annex A and the other models take into account the redistribution of stresses from the middle of the plate to the unloaded edges and therefore they should give higher value. The 6%

difference is also an indicator that the calculations carried out for the modules is reasonable as the plate behaviour should have column like behaviour due to the aspect ratio of the plate.

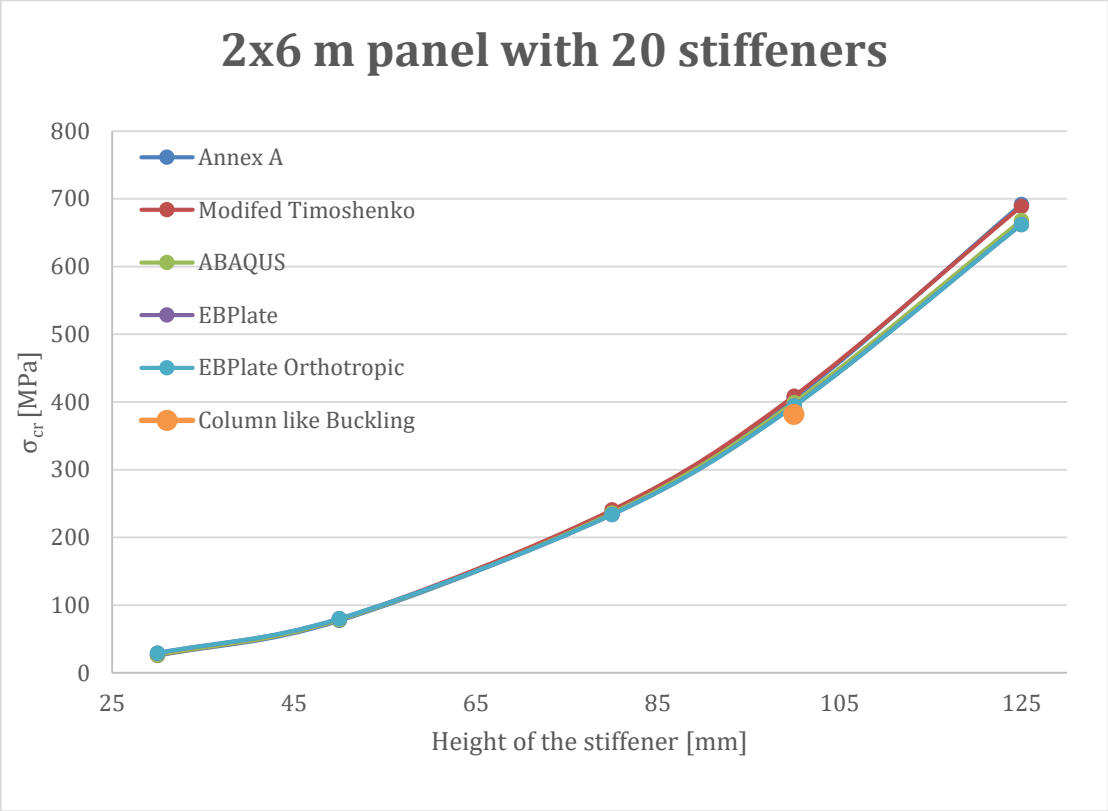

Figure 4.9. Results from all the different methods for stiffened panel D with various stiffener heights.

For panel D, the analytical solutions give almost the same results for all stiffeners while ABAAQUS and EBPlate are showing similar results. Even though the models are not showing exactly the same critical buckling stress the maximum difference is insignificant or around 3.5%.

As the stiffeners height increase the correlations between methods drift apart somewhat for all test plates. It does not matter if the plate is small (2x2 m) with sex or teen stiffeners or if you have larger plate (4x4 m) all methods will yield similar results. It also yields good results when it comes to the column-like buckling as shown in Figure 4.9. Therefore, it can be assumed that for the elastic critical buckling stress of a plate with simply supported boundary conditions on all edges, has at least three or more flat bar stiffeners with various height of stiffener and panel sizes, the critical buckling stress can be calculated with any of the method described before as they all yield similar results.

- All methods for all panels converge almost perfectly
- Plate-like behaviour, in panels A, B and C, is reflected well in all methods
- Column-like behaviour, in panel D, is reflected well with all methods
- The maximum difference between models for critical buckling stress is around 5%

5 Modelling and results for SSP

5.1 Introduction

In this chapter the modelling of SSP is the main objective, verify the modelling procedure and compare different methods with respect to elastic critical buckling stress. A great lack of published work specifically on buckling and steel sandwich panels meant that it would be hard to verify the end results. The finite element modelling would as well have to be verified with respect to some other aspect then buckling and then utilized for buckling analysis. In the light of day, most published work in the SSP was done with respect to deflection and therefore it was chosen to be the verification method for the modelling process.

Chapter five is split into four sub chapter where the first one is a general introduction and an overview of the chapters' content. Following the first chapter come two verification chapters 5.2 and 5.3, were 3D modelling and 2D equivalent modelling is verified respectively. In the last chapter the elastic critical buckling stress in analysed with three panels A, B and C with various cross-sections. The three panels are meant to check both the plate-like and column like behaviour and are analysed with an analytical method discussed in the literature chapter, EBPlate and both 3D and 2D finite element models.

5.2 3D modelling verification study (SSP 6x2.1m)

5.2.1 Introduction

This subchapter includes a study to verify a modelling technique with respect to deflection. The model that was chosen to model and verify is a 6x2.1m SSP panel with a corrugated web that was originally tested by Tan in 1989. Tan tested a specific panel with finite element analysis, close-form solution analytical method and with a physical experiment and compared all three with good results. Since then a number of papers have been published using the same SSP panel for comparison (Poirier et al., 2013) and (Chang et al., 2005). This panel is therefore an opportune option to use as a verification model and was therefore used.

5.2.2 Geometry and material properties

Herein the geometry and material properties of the SSP is discussed and explained. The panels' size is $6x2.1[m]$ with four corrugated cores running all the way through the long way around see Figure 5.1. Both facing sheets, the top one and the bottom one, have the same thickness of $2.5[mm]$. The web has the same thickness as the facing sheets $2.5[mm]$ see Figure 5.2. All around the panel there is an edge plate that closes the panels' edges. This edge plate had the thickness of $12[mm]$ in Tans experiment but for the sake of interest a small study was conducted to see the effect of various thicknesses of the edge plate, see subchapter 5.2.5.

The web was attached to the facing sheets with two spot welds along the entire length of the panel. In this verification study the spot welds where modelled as a continuous weld which caused a slight increase in stiffness which in turn decreased the deflection slightly. The edge plate was however continuously

welded all around the panel and should therefore be reflected well in the 3D model.

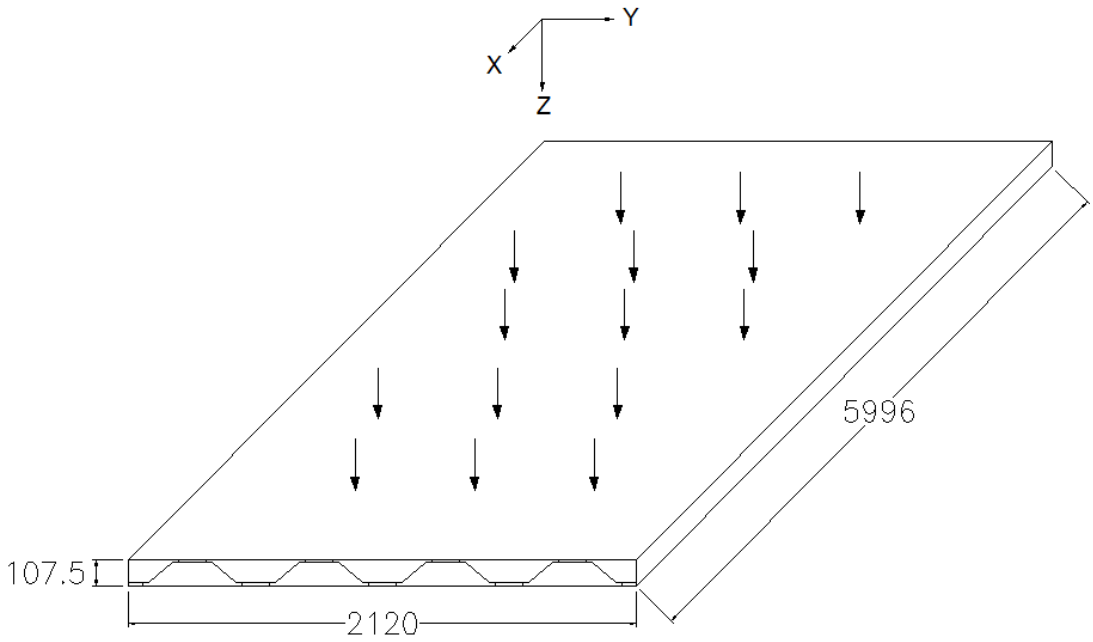

Figure 5.1 6x2.1 panel showing rough size and loading conditions.

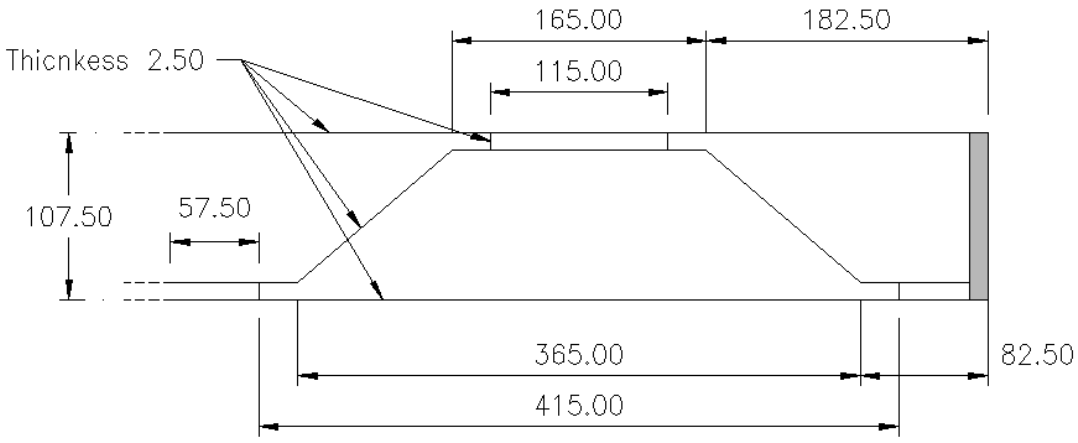

Figure 5.2. 6x2.1m panel cross-section details.

Material

The material properties of the steel used in Tans experiment was all of the same for all the parts of the SSP. Tan tested the steel before his experiment in tension and found out that the mean elastic modulus was 209[GPa] which is a bit lower than the traditional value of 210[GPa]. The yield strength of the steel was also tested and found to be 310[MPa]. For the testing of this 3D model the same material properties where used in order to compare too Tans results which are:

- Material Steel
- Young's modulus 209000 [MPa]
- Poisson's ratio 0,3 [-]

5.2.3 Modelling

The panel was modelled as a 3D structure in the finite element program ABAQUS. The cross section was modelled using shell elements were the web, top- and bottom-flange and welds where modelled with the thickness of 2.5mm. The edge plate was modelled as a shell as well and attached to the edges, covering the whole edge all around.

Loading and Boundary conditions

The panel was loaded in the same way as Tan with out of plane load in the entire top surface of the amount of 5.5[kN/m^2]. The plate was simply supported on all edges and the boundary conditions were applied at the bottom. It is notable that the coordinate system is officially like it is shown in Figure 5.1 but not as seen in Figure 5.3 taken from ABAQUS. The elements used in the modelling was chosen to be quadratic with 6 degrees of freedom in each node and 8 nodes per element. The model with all the boundary conditions and loading can be seen in Figure 5.3.

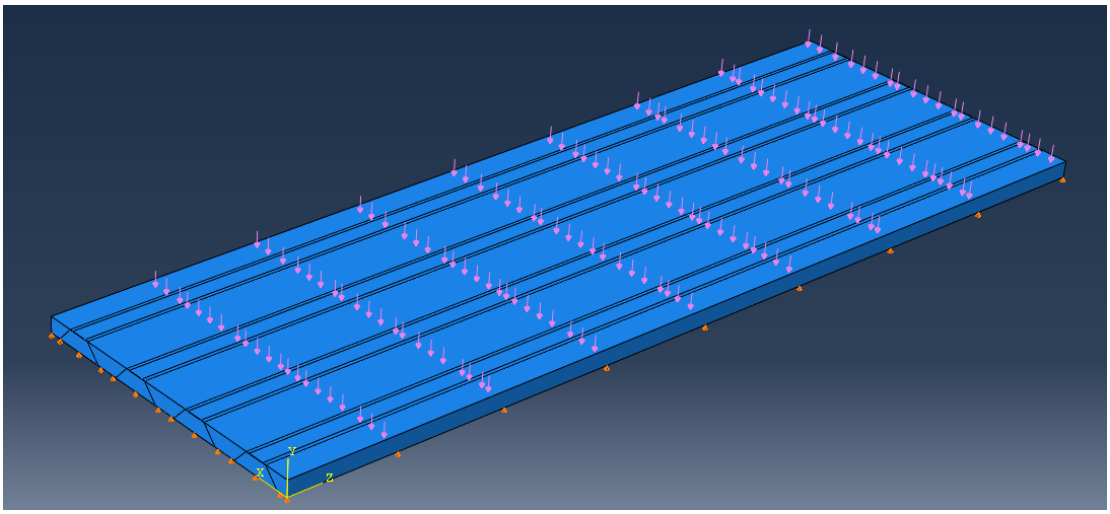

Figure 5.3. 6x2.1m panel modelled in ABAQUS showing loading and boundary conditions.

5.2.4 Convergence study

A conventional convergence study was performed to verify that the model converges. The convergence study was also used to estimate the number of elements needed for the model to be accurate enough. This study was done before the edge plate study so the original 12mm edge plate was used in this study. The results from the convergence study are stated in Table 5.1.

Table 5.1. Results from the convergence study done on the 6x2.1 [m] 3D ABAQUS model.

Element size [mm]	Top flange deflection [mm]	Bottom flange deflection [mm]	Average deflection [mm]	Difference [%]
300	*7,810*	*5,733*	*6,772*	
200	*7,811*	*5,733*	*6,772*	*-0,03%*
150	*7,814*	*5,737*	*6,776*	*-0,17%*
100	*7,815*	*5,736*	*6,776*	*0,00%*
80	*7,816*	*5,737*	*6,777*	*-0,05%*

The results from the convergence study clearly show that the model converges towards a correct solution. Using element size from 300-100 all give really similar results with all differences under one percentage. The highest difference is between the size 200 and 150 which is only 0.17%.

5.2.5 Edge plate study

This edge plate study was made not out of necessity but more out of curiosity and with the buckling analysis in mind. Later on in the buckling analysis the load would no longer be out of plane load on the top surface but rather in-plane load on the edge. With that in mind the idea of the convenience of being able to increase the edge plate thickness in order to get better stress distribution, hopefully without a large effect on the behaviour, arose. The edge plate study was done by decreasing the edge plate by half, increasing it by doubling it and so forth. The result was as we had hoped, a relatively small difference about 1-2 percent was obtained between tests. The results from the study can be seen in Table 5.2.

Table 5.2. Results from an edge plate study done on a 6x2.1m 3D model in ABAQUS.

Edge plate thickness [mm]	Top flange deflection [mm]	Bottom flange deflection [mm]	Average deflection [mm]	Difference [%]
6	*7,924*	*5,844*	*6,884*	
12	*7,815*	*5,736*	*6,776*	*1,58%*
18	*7,772*	*5,696*	*6,734*	*0,61%*
24	*7,730*	*5,655*	*6,693*	*0,62%*
30	*7,694*	*5,630*	*6,662*	*1,53%*

5.2.6 2D equivalent model

In this study the main emphasis was on the 3D modelling but an equivalent 2D plate was also modelled using the method from the next subchapter 5.3. The modelling technique is explained in the following chapter but in Table 5.3 the stiffness parameters used in this study are given.

Table 5.3. 6x2.1m panel, equivalent stiffness parameters and the converted once for general shell stiffness model.

D_x [Nm]	D_y [Nm]	D_{xy} [Nm]	D_{Qx} [N/m]	D_{Qy} [N/m]	E_x [N/m]	E_y [N/m]	G_{xy} [N/m]
4,32E+06	*3,24E+06*	*2,43E+06*	*2,96E+07*	*1,59E+05*	*1,66E+09*	*1,08E+09*	*5,74E+08*

D_{11} [Nm]	D_{12} [Nm]	D_{22} [Nm]	D_{33} [N/m]	D_{44} [N/m]	D_{55} [N/m]	D_{45} [N/m]	D_{66} [N/m]
1,76E+09	*3,45E+08*	*1,15E+09*	*5,74E+08*	*4,63E+06*	*3,47E+06*	*1,04E+06*	*1,22E+06*

5.2.7 Results

This study was made to verify the modelling technique for a 3D SPP panel with respect to deflection. The result from the 3D model conducted in ABAQUS is then compared to published results from modelling and testing. Maximum deflection of the top- and bottom flange and the average of the two is found and compared. The maximum deflection is found at the centre of the panel see Figure 5.4. The results from this current analysis and numerous published results are stated in Table 5.4.

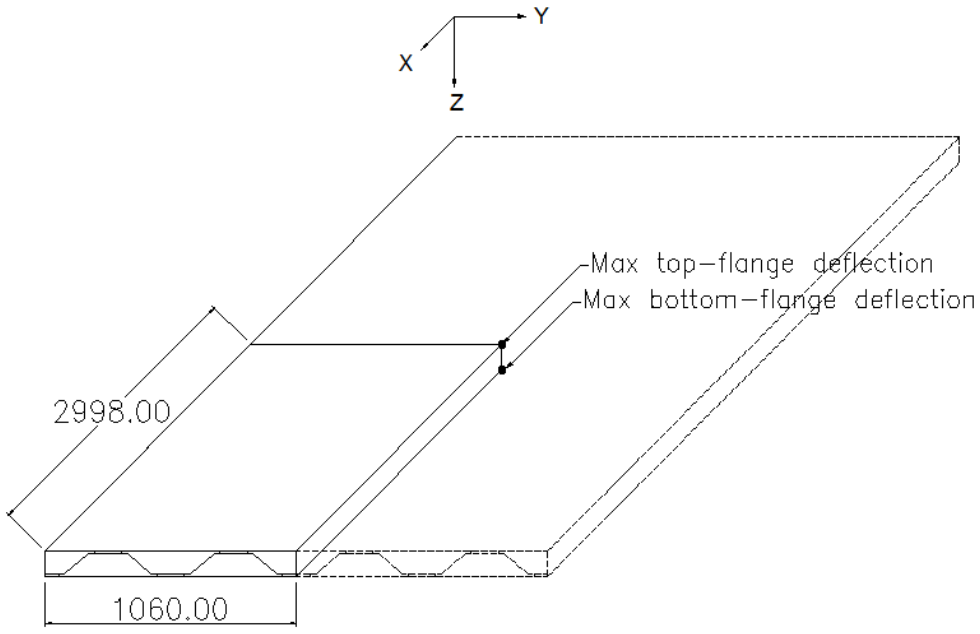

Figure 5.4. 6x2.1m panel showing the locations of maximum deflection of the panel.

The deflection is either an average maximum deflection or the maximum deflection in the top flange and bottom flange this difference can be seen in Figures 5.5 and 5.6. The 2D equivalent model and all analytical methods only give the average deflection which raises the problem of comparing that deflection to the 3D model. One way of comparing the two is to find the maximum deflection of the bottom flange and the maximum deflection in the top flange and compare the average of two to the average value found in the 2D model and analytical method (Poirier et al., 2013).

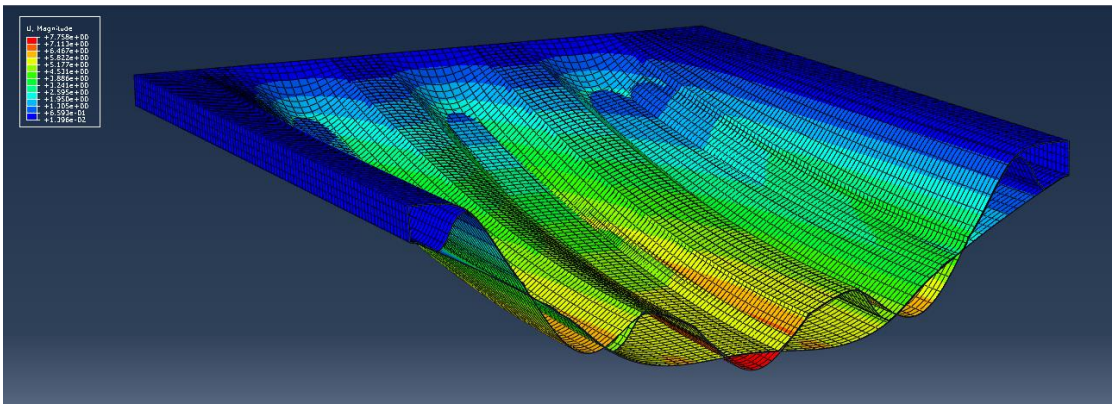

Figure 5.5. 6x2.1m panel deflection results from 3D modelling in ABAQUS.

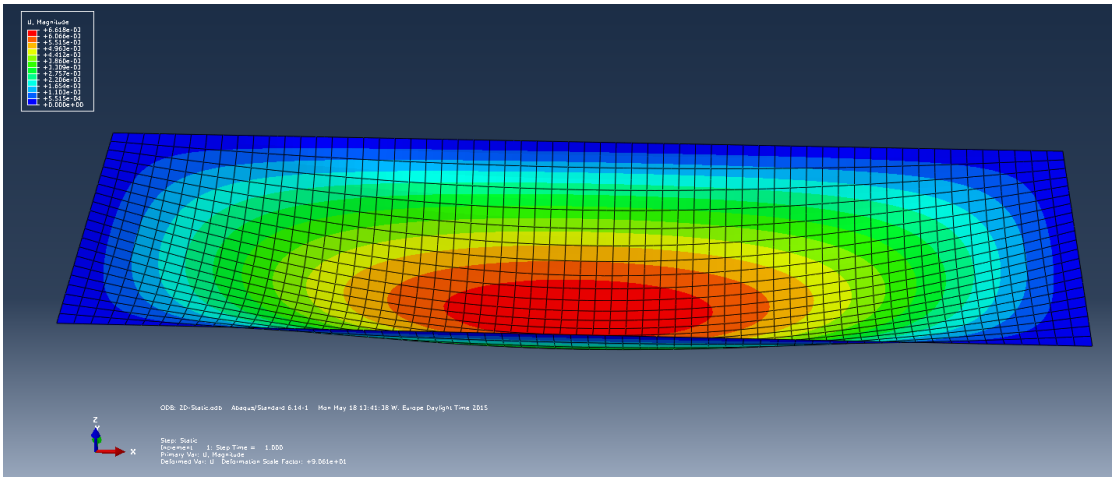

Figure 5.6. 6x2.1m panel deflection results from 2D modelling in ABAQUS.

Table 5.4. 6x2.1m deflection results from published and present results.

Analysis	Avarage deflection [mm]
Results from publisehd studies	
Lok and Cheng, Analytical study	6,86
Lok and Cheng, FE study	6,78
Cheng, Analytical	6,75
Multi-objective	6,98
Results from present study	
Present FE 3D model	6,78
Present FE 2D model	6,62

Compering the present solution to previously published work the correlation is clear from table 5.4. The 3D solution is exactly the same as Lok & Cheng Fe study and the rest is similar as well. The 2D solution is a little bit lower but it is an approximation so some small difference can be expected. In whole this is a really good result which strongly indicates that the modelling technique for both the 3D and 2D equivalent model give correct results at least with respect to deflection.

Variations between publishers

Some minor differences are between the different researchers for example is the load varying between $5.5[kPa/m^2]$ and $5.52[kPa/m^2]$. As well is it not clear between authors what they refer to as h_c either it is taken as the height between centre to centre of the top flanges or the inner flanges. Likewise is the E-modulus either taken as 209 or 208 $[GPa]$ and these differences can be the source of errors that can explain the small difference between results.

5.3 2D equivalent plate deflection (6x2.1m)

5.3.1 Introduction

In this chapter a verification of 2D equivalent modelling technique published by (Chang et al., 2005) is conducted. As was discussed in the literature study chapter, Cheng based his modelling on the Mindlin-Reissner plate theory and idealized a corrugated sandwich 3D structure as an equivalent 2D homogeneous orthotropic thick plate structure. In order to do so he utilizes the stiffness parameters that Libove and Hubka derived in 1951. In total 27 panels (A1-A27) from the study Cheng made in 2005, where computed in the finite element program ABAQUS and compared to the close-form solution from the matched optimisation routine which was discussed in section 2.4.3.

5.3.2 Geometry

In Chengs parametric study he always models the same 6x2.1 [m] panel but with different corrugated-core configurations. The core depth is kept constant $(h_c = 0.1m)$ and the core sheet to face sheet thickness is also kept constant $(h_c/t_c = 20)$. Cheng conducted a numerical investigation with certain ratios ever changing $\alpha, t_c/f_c \; and \; p/h_c$.

The results from Chengs parametric study was given up in two tables, in the first table ($h_c = 0.1m$) and ($h_c/t_c = 20$) was kept constant in the second table these constants where increased. In this verification study it was considered enough to use the first table. In the present study the first table except for corrugation angle 90° was modelled. The geometrical constants that describe the corrugated core can be seen in Figure 5.7. The geometry of a sandwich can be described with a few geometrical constants as was discussed in the literature chapter. The test subjects, in this study, geometrical constants are stated in Table 5.5 and in Figure 5.8 the geometrical constants are explained.

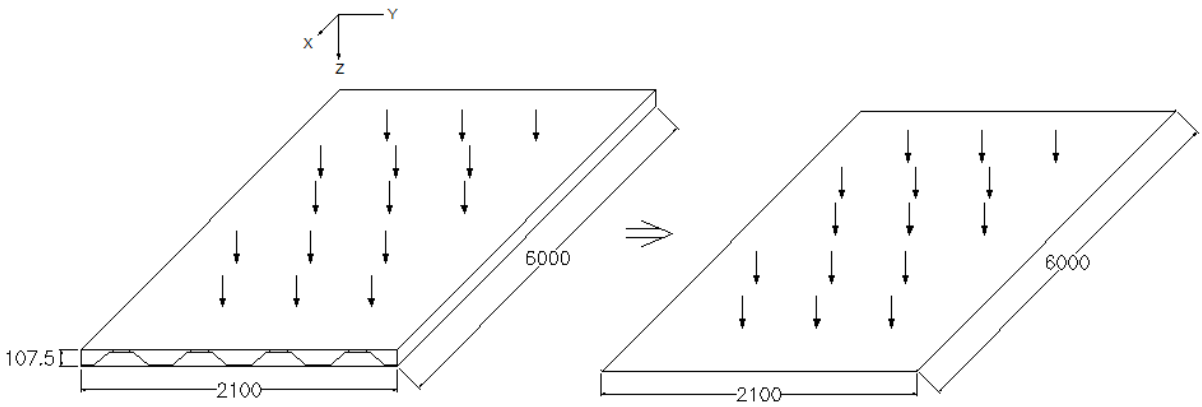

Figure 5.7. 6x2.1m panel converted from a 3D- to a 2D-structure showing loading and coordinate system.

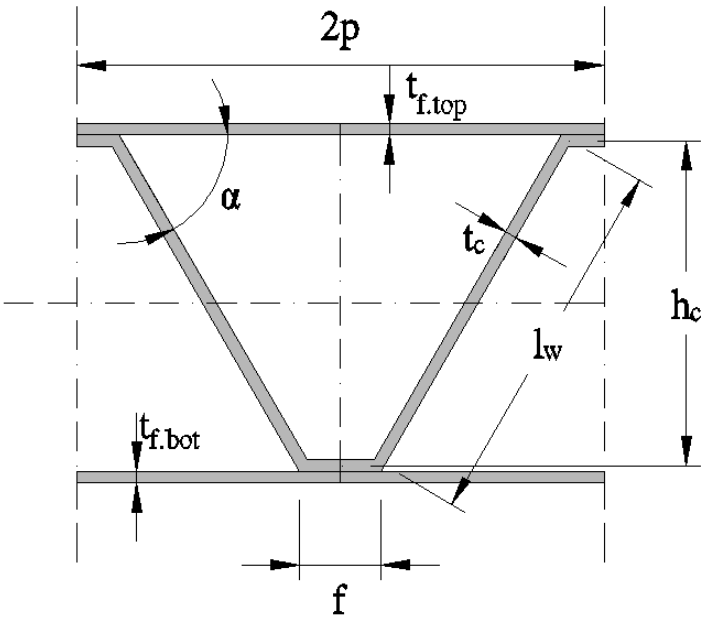

Figure 5.8. Cross-section of corrugated-core panel showing its geometrical constants.

Table 5.5. Geometrical constants of the tests subjects in the 2D equivalent model verification study.

Panel nr.	h_c [mm]	t_c [mm]	α [deg]	t_f [mm]	t_c/t_f	p [mm]	p/h_c
A1	*100*	***5***	*60*	*8,3*	*0,6*	*100*	*1*
A2	*-*	*-*	*-*	*8,3*	*-*	*120*	*1,2*
A3	*-*	*-*	*-*	*8,3*	*-*	*140*	*1,4*
A4	*-*	*-*	*-*	*5,0*	*1*	*100*	*1*
A5	*-*	*-*	*-*	*5,0*	*-*	*120*	*1,2*
A6	*-*	*-*	*-*	*5,0*	*-*	*140*	*1,4*
A7	*-*	*-*	*-*	*4,0*	*1,25*	*100*	*1*
A8	*-*	*-*	*-*	*4,0*	*-*	*120*	*1,2*
A9	*-*	*-*	*-*	*4,0*	*-*	*140*	*1,4*
A10	*-*	*-*	*70*	*8,3*	*0,6*	*100*	*1*
A11	*-*	*-*	*-*	*8,3*	*-*	*120*	*1,2*
A12	*-*	*-*	*-*	*8,3*	*-*	*140*	*1,4*
A13	*-*	*-*	*-*	*5,0*	*1*	*100*	*1*
A14	*-*	*-*	*-*	*5,0*	*-*	*120*	*1,2*
A15	*-*	*-*	*-*	*5,0*	*-*	*140*	*1,4*
A16	*-*	*-*	*-*	*4,0*	*1,25*	*100*	*1*
A17	*-*	*-*	*-*	*4,0*	*-*	*120*	*1,2*
A18	*-*	*-*	*-*	*4,0*	*-*	*140*	*1,4*
A19	*-*	*-*	*80*	*8,3*	*0,6*	*100*	*1*
A20	*-*	*-*	*-*	*8,3*	*-*	*120*	*1,2*
A21	*-*	*-*	*-*	*8,3*	*-*	*140*	*1,4*
A22	*-*	*-*	*-*	*5,0*	*1*	*100*	*1*
A23	*-*	*-*	*-*	*5,0*	*-*	*120*	*1,2*
A24	*-*	*-*	*-*	*5,0*	*-*	*140*	*1,4*
A25	*-*	*-*	*-*	*4,0*	*1,25*	*100*	*1*
A26	*-*	*-*	*-*	*4,0*	*-*	*120*	*1,2*
A27	*-*	*-*	*-*	*4,0*	*-*	*140*	*1,4*

5.3.3 Stiffness parameters

The stiffness parameters used in this study, as was stated in the literature study, where derived by using a optimisation routine developed by Beneus and Koc in 2014. This routine was further developed by (Dackman & Ek, 2015) taking into account different top and bottom face sheet thicknesses. Equations for the stiffness parameters are stated and discussed in section 2.4.3.

The torsional stiffness's D_{Qx} *and* D_{Qy} where found be slightly different from the once Cheng used in 2005(Dackman & Ek, 2015).. A study was made to compare the deflection received using the improved torsional stiffnesses compared to the

deflections Cheng found in his study. The results from this can be found in the appendix.

5.3.4 Modelling

To model the 3D sandwich plate structure as an equivalent 2D plate the stiffness parameters are used to add stiffness to a simple 2D shell element with the same length and width as the original panel. To do this in ABAQUS there are various different options of utilizing the stiffnesses for example the lamina model, orthotropic model and the general shell stiffness.

The orthotropic modelling option was not tested because to many variables where needed which were unknown. Lamina modelling option was found to be ineffective when both in-plane and out-of-plane loading was applied at the same time and therefore excluded. General shell element modelling option was found be the most appropriate for the task taking both in-plane and out-of-plane loading into account at the same time and all variables where known. Furthermore, testing yielded good results both for deflection and buckling analysis.

In the general shell element modelling option, stiffness is given directly to the plate by inputting stiffness factors derived from the stiffness parameters directly into the stiffness matrix. How these stiffness factors (D_{11}, D_{12} , D_{22} , D_{33}, D_{45}, D_{44} , D_{55} , D_{66}) are derived is explained in the literature chapter under general shell stiffness. In the literature chapter a further discussion on how these stiffnesses are applied in the general shell stiffness model.

Boundary conditions that Cheng used were of the type hard type simply supported. This means that all on top of all edges being simply supported, meaning fixed in the vertical direction, as well fixed with respect to rotation in the same direction as the edge lies. The boundary conditions are explained in Figure 5.9 and stated here below:

- All four edges are fixed in the z-direction.
- Both short edges (loaded edges) have rotation fixed about the x-axes.
- Both long edges (unloaded edges) have rotation fixed about the y-axes.
- The entire plate surface is loaded with out-of-plane pressure of the magnitude $10[kN/m^2]$.

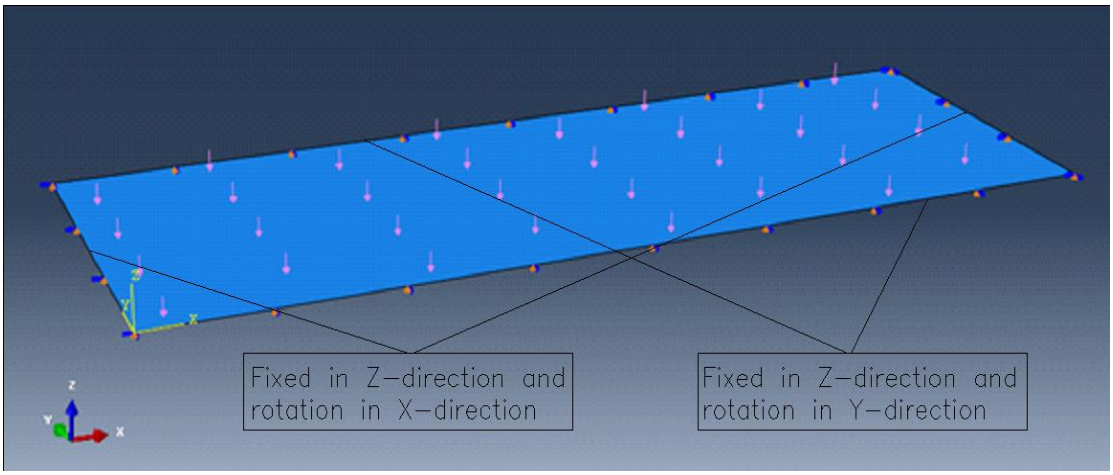

Figure 5.9. 6x2.1m, 2D-equivalent plate showing boundary conditions and loading in ABAQUS.

5.3.5 Convergence study

A convergence study was conducted to verify that the solution converged towards a correct solution. The result was that extremely large elements yield the exact same solution as really fine once see Table 5.6.

Table5.6. Results from a convergence study conducted on a 2D equivalent model, panel 6x2.1m.

Element size [mm]	Average deflection [mm]	Difference [%]
500	*0,338*	
300	*0,338*	*0,00%*
100	*0,338*	*0,00%*

5.3.6 Results

The results from this study were good as can be seen in Figure 5.10 where the deflection from the analytical method and the 2D equivalent finite element analysis are compared. An example of the deflection analysis is shown in Figure 5.11 where panel A1 is tested in ABAQUS. The difference between the two analyses is in all cases below one percent which is reflected in the figure where the results completely overlap.

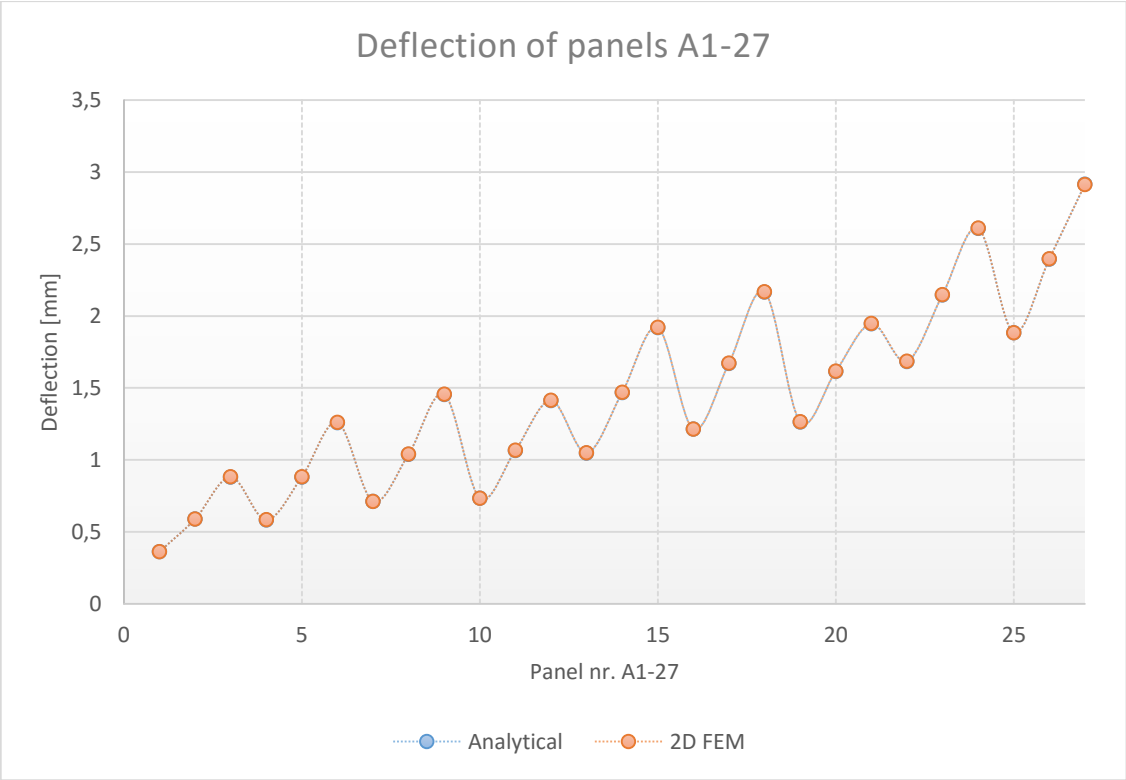

Figure 5.10. Results from a deflection study where an analytical method and FEM analysis for 27, 2D equivalent panels are compared.

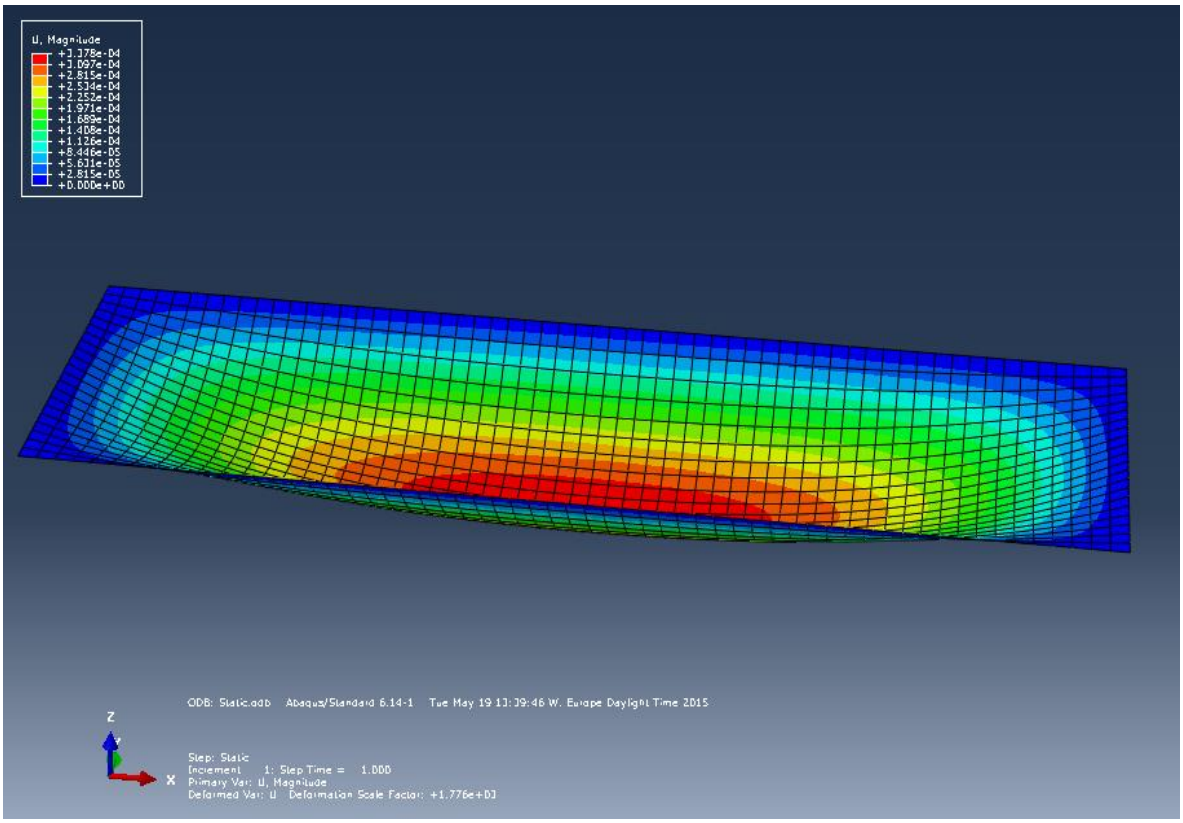

Figure 5.11. 6x2.1m panel deflection as 2D plate with $h_c = 0.1m$, $h_c/t_c = 20$, α=60°, $t_c/t_f = 0.6$, $p/h_c = 1$.

5.4 Buckling analysis of panels A, B and C

5.4.1 Introduction

In this chapter 3D and 2D FEM analysis, analytical method and EBPlate where used to analyse three panels with the aim of estimating the critical buckling stress. The objective was to compare and conclude from the difference between the different methods and conclude an easy way of calculating the critical buckling stress for global buckling. In order to force global buckling to occur the cross-section was designed to have all parts of the cross-sectional in cross-sectional-class 3 or lower.

The size of the three panel was chosen in order to verify both plate-like and column-like behaviour. Similarly, as was done in the stiffened plate analysis it is important to see how well all the methods take these two effects into account. By having an aspect ratio close to one or above the panel will buckle like a plate but by having the plate wide and short the centre part will not gain any post-critical strength from the tension cord and will buckle almost like a column.

The panels were first verified with respect to deflection with out-of-plane load like before in the previous chapters to verify that the models are behaving correctly with respect to structural abilities. All three panels that were analysed can be seen in Figure 5.12.

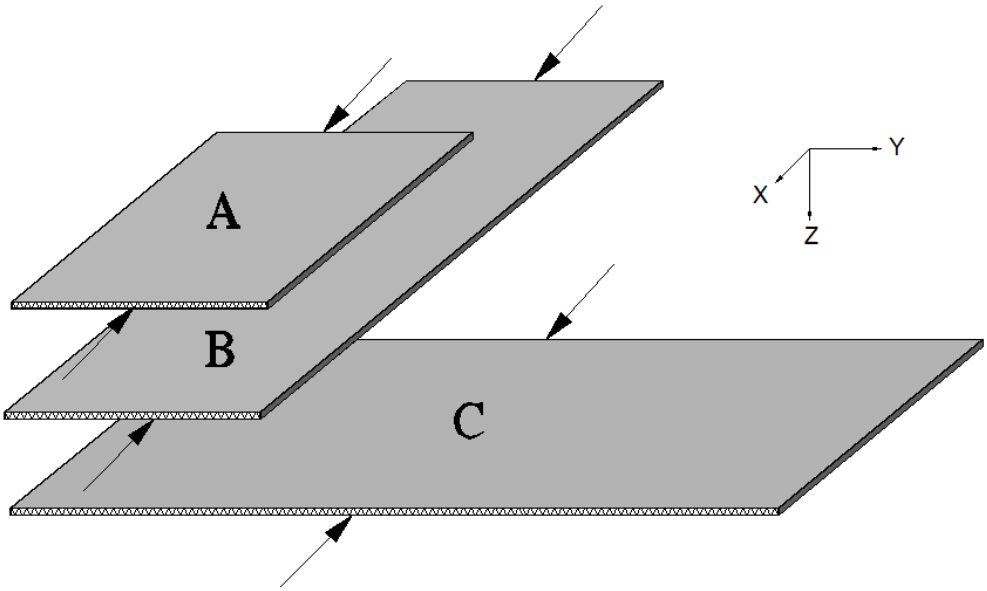

Figure 5.12. Steel sandwich panels A, B and C, using in the buckling analysis.

5.4.2 Geometry

All three panels A, B and C have got a different way of buckling because of their size and aspect ratio see table 5.1. Panel A has an aspect ratio close to 1 and will therefor buckle in a plate like behaviour in one half sinus-wave. Panel B has an aspect ratio of 3 and will therefore buckle in plate-like-behaviour and buckle in three half-sinus-waves. Panel C is short and wide with an aspect ratio of 1/3 and

will therefore buckle in its centre almost like a column before the tension cord can form between the two unloaded edges.

Each of the panels was tested with six variations of cross-section where the top- and bottom-face-sheet and web thickness are variable. The cross-section for panel A1, B1 and C1 is therefore the same and is shown in Figure 5.13.a. In Figure 5.13.b the explicit way the cross-section was modelled in ABAQUS where all lengths are explicitly shown. It should be noted here that the welds between the web and the face-sheets are also modelled as shell elements which causes added stiffness which is not included in the 2D equivalent model. A small study was made to check the effect of this added stiffness and the result from that can be seen in the literature study. The cross-sections are all in cross-sectional class 3 or lower in order to exclude local buckles to occur. All six variations of cross-section can be seen in Table 5.7 and the geometrical constants and stiffness parameters are shown in Table 5.8 and Table 5.9 respectively.

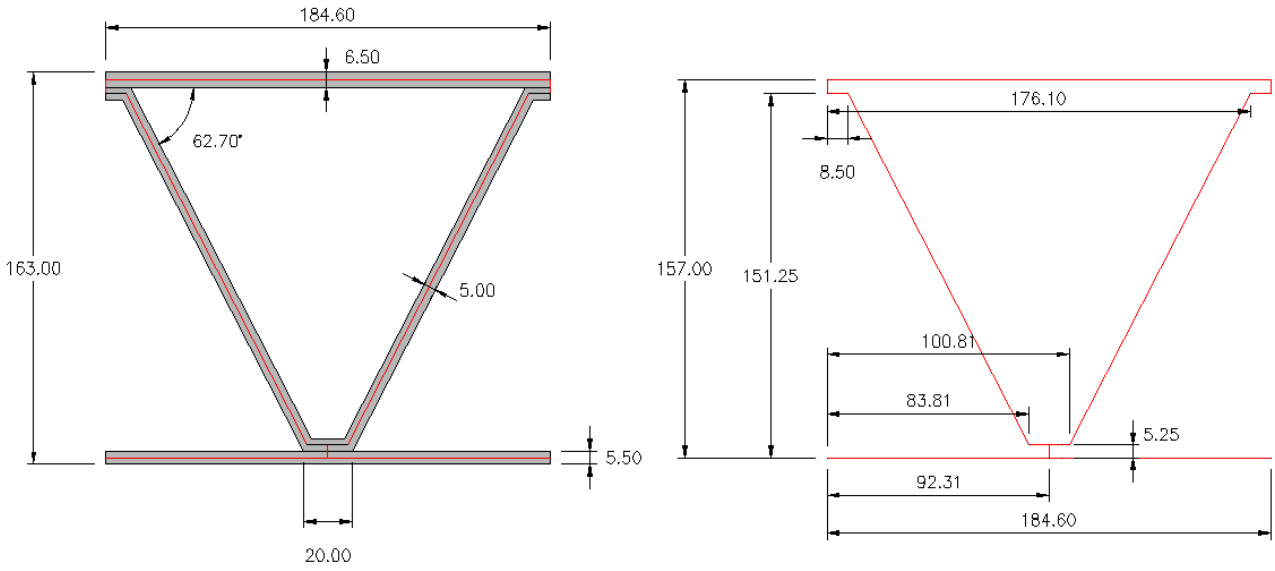

Figure 5.13. a) Cross-section of panel A1, B1 and C1 b) How the cross-section is modelled in ABAQUS.

Table 5.7. Panels A, B and C relative size and aspect ratios.

Panel nr.	Length [m]	Width [m]	Aspect ratio
A	*8*	*6*	*1,33*
B	*18*	*6*	*3,00*
C	*6*	*18*	*0,33*

Table 5.8. Panels A, B and C geometrical constants.

Panel nr. A,B,C	h_c [mm]	$t_{f.top}$ [mm]	$t_{f.bot}$ [mm]	tc [mm]	α [deg]	f [mm]
1	*146*	*6,5*	*5,5*	*5*	*62,7*	*20*
2	*146*	*8*	*5,5*	*5*	*62,7*	*20*
3	*146*	*8*	*8*	*5*	*62,7*	*20*
4	*146*	*8*	*8*	*7*	*62,7*	*20*
5	*146*	*6,5*	*5,5*	*7*	*62,7*	*20*
6	*146*	*7,5*	*6,5*	*5*	*62,7*	*20*

Table 5.9. Panels A1, B1 and C1 corresponding 2D equivalent stiffness parameters.

Panel nr. A,B,C	D_x [Nm]	D_y [Nm]	D_{xy} [Nm]	D_{Qx} [N/m]	D_{Qy} [N/m]	E_x [N/m]	E_y [N/m]	G_{xy} [N/m]
1	*1,99E+07*	*1,58E+07*	*1,19E+07*	*5,67E+08*	*1,10E+08*	*4,55E+09*	*2,63E+09*	*1,18E+09*
2	*2,17E+07*	*1,94E+07*	*1,46E+07*	*5,77E+08*	*1,11E+08*	*4,86E+09*	*2,95E+09*	*1,30E+09*
3	*2,56E+07*	*2,16E+07*	*1,63E+07*	*5,81E+08*	*1,45E+08*	*5,39E+09*	*3,48E+09*	*1,50E+09*
4	*2,79E+07*	*2,22E+07*	*1,68E+07*	*8,34E+08*	*2,84E+08*	*6,20E+09*	*3,51E+09*	*1,59E+09*
5	*2,20E+07*	*1,63E+07*	*1,22E+07*	*8,13E+08*	*2,31E+08*	*5,36E+09*	*2,65E+09*	*1,63E+09*
6	*2,27E+07*	*1,86E+07*	*1,41E+07*	*5,74E+08*	*1,28E+08*	*4,97E+07*	*3,05E+09*	*1,34E+09*

5.4.3 3D Modelling

To estimate the critical buckling stress of the panels' linear eigenvalue buckling analysis is performed for all the panels using Lanczos eigenvalue solver under uniform edge displacement. This process is much like the buckling analysis done for the stiffened plate with small variations. To find a prediction of the global buckling stress a static analysis must be run first and the sectional stress extracted which is called the reference critical buckling stress (σ_{ref}). The same model was then run through linear buckling analysis using Lanczos eigenvalue solver and for the global buckling mode the reference eigenvalue (λ_{ref}) is found. The algorithm in ABAQUS solves the linearized eigenvalue problem

$$(K - \lambda K_G)\phi = 0 \qquad (5.1)$$

Given that the panel buckles globally the multiplication of the two reference values gives the critical buckling stress for the global buckling mode. The first buckling mode is often the global one but not always.

$$\sigma_{cr} = \sigma_{ref} \cdot \lambda_{ref} \qquad (5.2)$$

Ideally the stress over the whole cross-section should be the exact same and no stress-raisers in the corners and that was the aim and as well one of the challenges modelling the steel sandwich plate. To achieve this is hard in ABAQUS for it is easy for local buckles to occur if the compression is not completely uniform or if there

are any elements not fully attached. The SSP geometry makes the modelling process difficult and easy to get local buckles.

A number of minor sources of errors and idealization differ between modelling in 3D and 2D take place in this modelling process. The courses that were considered are the following:

- Weld between web and flange adds stiffness in the 3D model but does not exist in the 2D model
- Shell elements will not fit perfectly when they meet under an angle which happens in the web. This might cause a slight less stiffness in the 3D model compared to the 2D model
- Unpredictable behaviour difference between a full 3D structure and the 2D equivalent model.

These courses of errors are discussed and estimated in the literature study chapter.

The main difference between this model and the one in chapter 5.2, where deflection is analysed by loaded with out-of-plane pressure, is that this one has to be loaded in-plane with displacement for the buckling analysis. The panel is loaded by displacement of 10mm in the same direction as the corrugation in order to analyse the buckling behaviour.

An attempts was made to analyse the buckling of the panels loaded perpendicular to the corrugation direction. That analysis revealed that the panels always buckled locally in that situation, even when the flange thicknesses and the web had been increased to 25mm. It was concluded that no need for global buckling analysis were needed for those cases because the failure mode would always be local buckle rather than global buckling.

In order to model the 3D and 2D as alike as possible, the whole edge should be compressed to have the whole cross-section in pure compression. At the same time the edge should be able to rotate which it cannot if the entire edge is loaded. There are ways of modelling the edge load on the whole area and make it acts in the centre allowing the edge to rotate, coupling and master slave node for example. These ways did not work in the buckling analysis so the end result was to use displacement at the centre of the edge plate see Figure 5.14. The stress distribution in the cross-section was inspected, it was concluded that some minor irregularities are around the edge but evens out and is even for most of the panel.

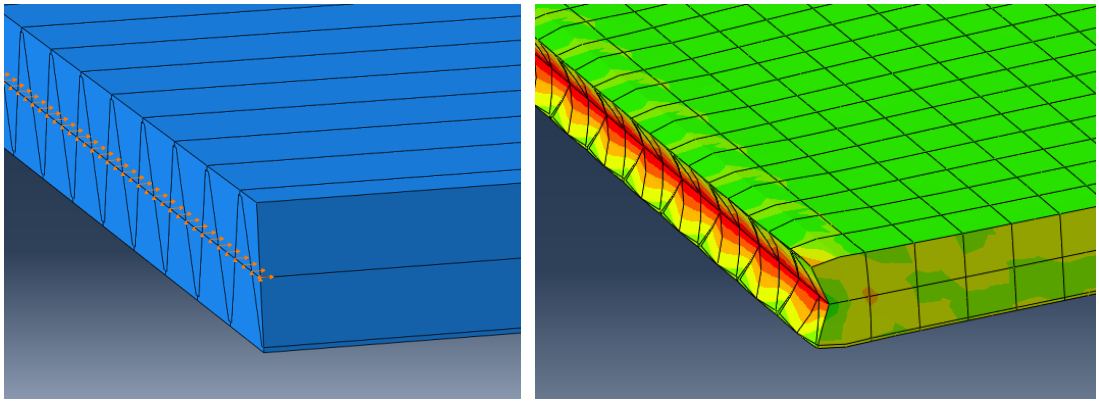

Figure 5.14. 3D modelling of panels A, B and C, a) displacement applied to the edge b) stress distribution in static analysis.

A convergence study was performed for both the 3D and 2D models which revealed the exact same result as the once done in previous studies in chapters 5.2 and 5.3. Therefore, it was not shown here rather referred to in previous chapters.

5.4.4 2D equivalent modelling

The 2D modelling process is basically the same as in chapter 5.3 for the deflection analysis except for the boundary conditions and loading. In the critical buckling analysis the boundary conditions are changed and the plate is now loaded with edge displacement instead of out-of-plate pressure. The stiffness is added to the plate like before with the general stiffness option. Hard type simply supported boundary conditions are used like before but also the edge counter to the loaded on has to be fixed in load-direction, the loaded plate can be seen in Figure 5.15.

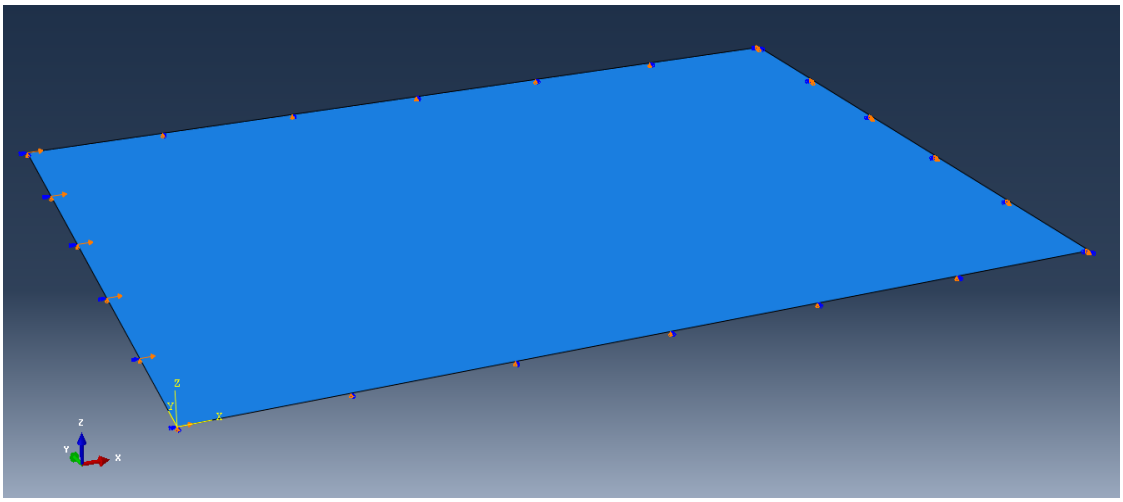

Figure 5.15. 2D equivalent plate modelled in ABAQUS showing all boundary conditions and loading.

Boundary conditions in Figure 5.15 are the following:

- All edges: Fixed in z-direction
- Long edges: Fixed rotation around y-direction

- Short edge1: Fixed rotation about x-axes and displacement of 10mm in x-direction
- Short edge 2: Fixed in the x-direction

5.4.5 Results

Before running the buckling analysis a deflection tests was made on all panels much like was done in chapter 5.3. The deflection analysis where compared between 2D equivalent FE model, 3D FE model and the analytical method used in chapter 5.3. Out of plane loading was used just like before. The results for each panel A, B and C can be seen in Figures 5.16, Figure 5.17 and Figure 5.18.

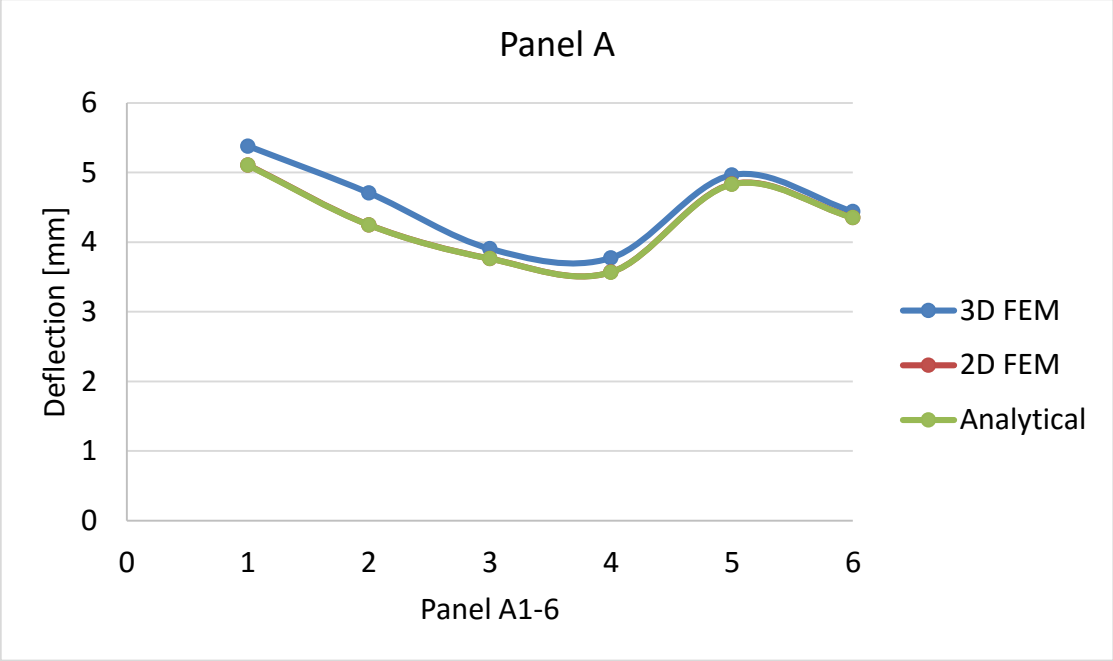

Figure 5.16. Deflection results for panel A1-6.

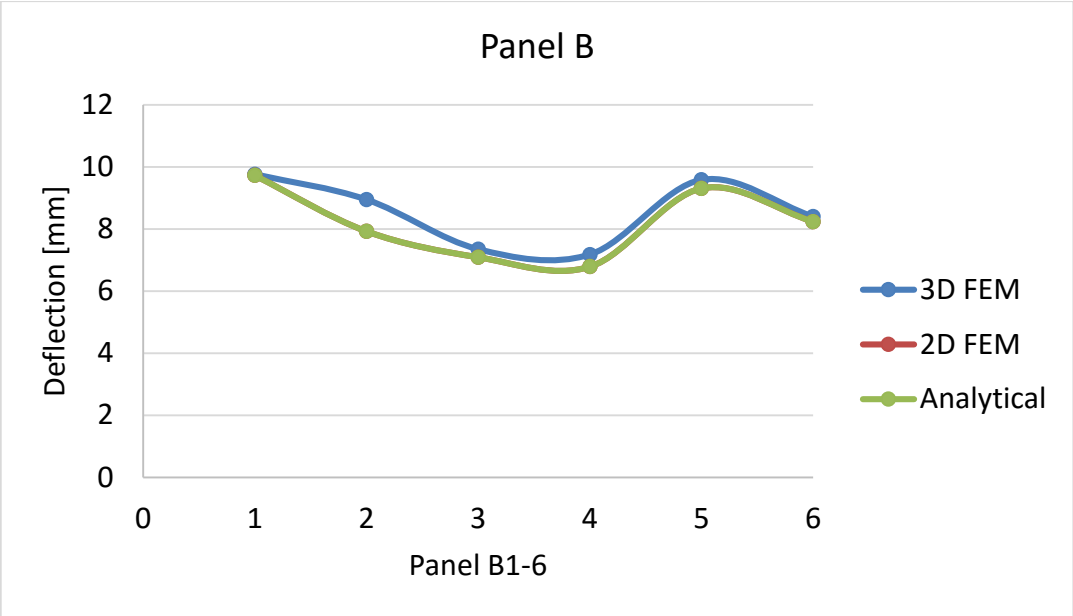

Figure 5.17. Deflection results for panel B1-6.

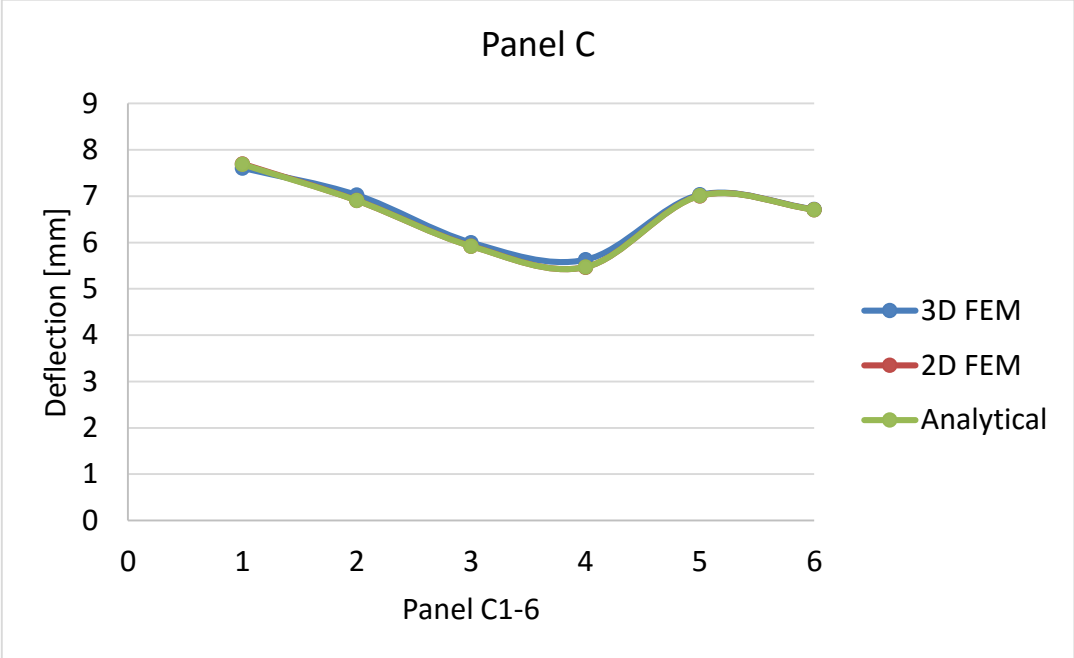

Figure 5.18. Deflection results for panel C1-6.

Deflection behaves give a strong indication of how well the FE models are working. The analytical method and 2D equivalent model should behave really similarly and as can be seen in the graphs they completely overlap like before in chapter 5.3. Comparing the 2D equivalent model and analytical method to the 3D FE model, in all cases the deflection of the 3D model is slightly higher but still follows the other two results closely. The deflection difference can be explained by local deflections in the face-sheets. Overall behaviour of the three models is similar and is therefore a strong indicator that the models are all working as they should.

The critical buckling stress was found and compared between 2D equivalent FE model, 3D FE model, EBPlate and the analytical method discussed in chapter 2.4.7. The result from the buckling analysis was the critical buckling stress and are shown for panels A, B and C in Figure. 19, Figure 20, and Figure 21 respectively.

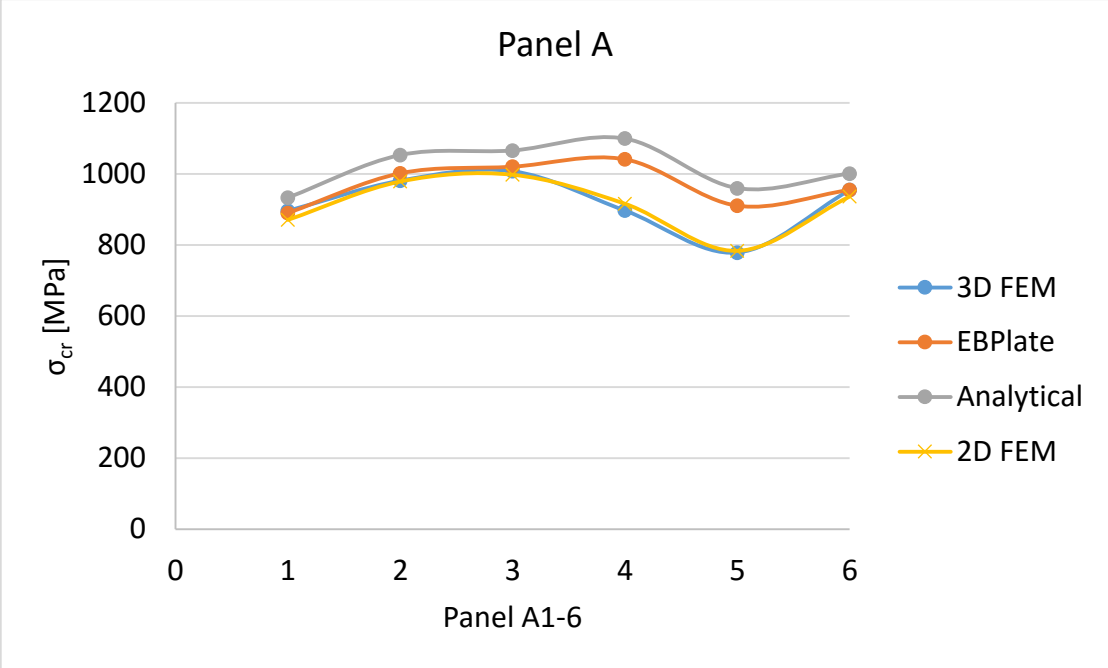

Figure 5.19. Results from buckling analysis of panel A1-6.

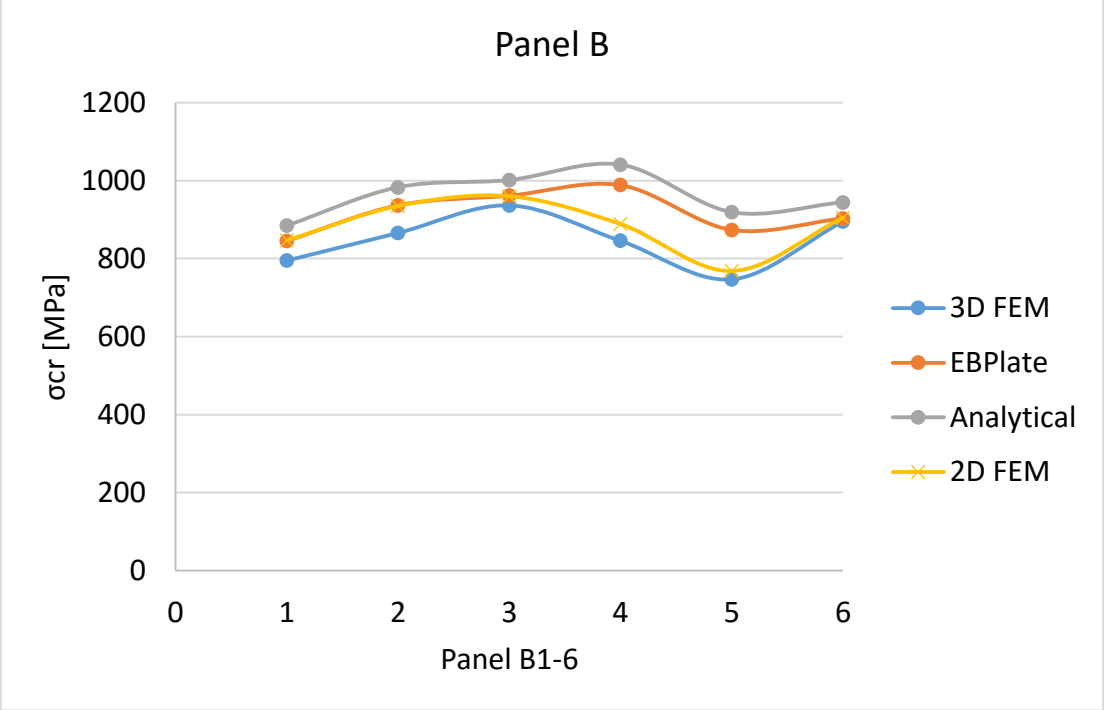

Figure 5.20. Results from buckling analysis of panel B1-6.

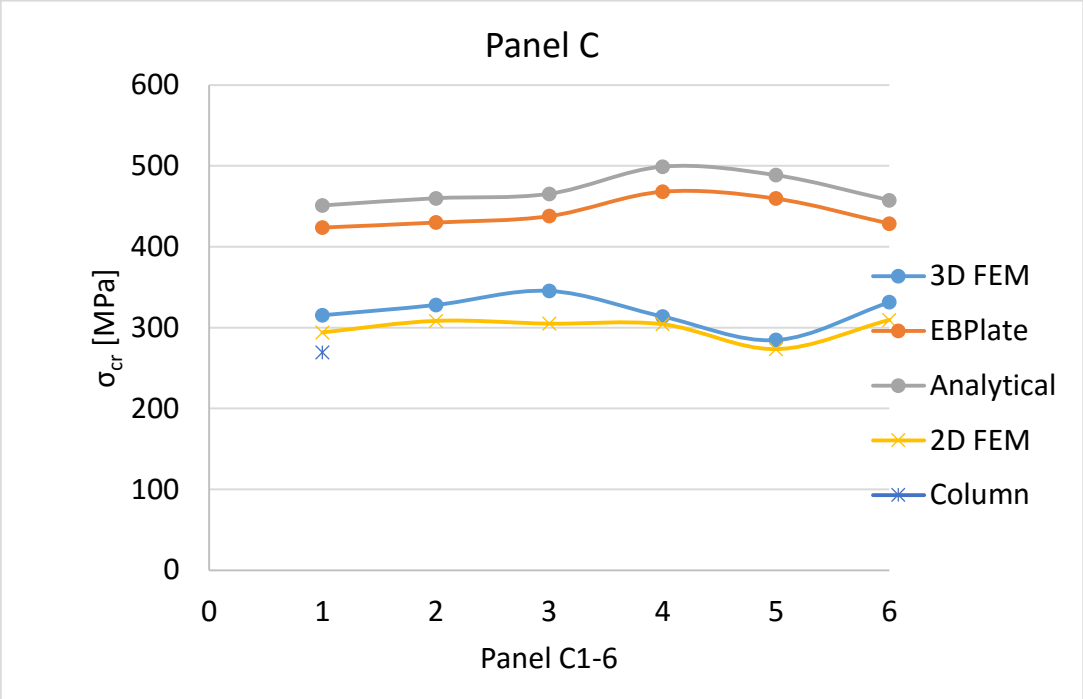

Figure 5.21. Results from buckling analysis of panel C1-6.

A number of results can be reasoned from the critical buckling stress analysis of panels A, B and C.

- In cross-section variations 4 and 5 where the web thickness is increased, for all panels, an unexpected drop in critical buckling stress was observed in the finite element models. This drop was not fixed or figured out but two observations where made which indicate where the problem may lay:
    1. By increasing one stiffness parameter one at a time and run the buckling analysis in the 2D equivalent model showed that when the axial stiffness E_x increased then the critical buckling stress decreased. It should be noted that the stiffness parameters are dependent on each other and in this test that connection was neglected completely.
    2. The only common modelling option between the two FE models is the how the boundary conditions are applied. This strongly indicated that the boundary conditions could be the problem.

- In core variations 1, 2, 3 and 6 where the core is constant and the flanges are increased the results are all similar. The two FE models and EBPlate

yield a weary similar result while the less accurate analytical model gives somewhat higher critical buckling stress in all cases.

- Panel C which buckles like a column rather than a plate yields an interesting results where EBPlate and the analytical models both yield a lot higher critical buckling stress, close to 200% of the FE models. The FE models however yield similar results.

- A small confirmation study was made to see how close the panel was to buckle like a column. From chapter 1 the critical buckling stress for a columns is used to compare to the FE models. 1m part of panel C1 is used as a test subject:

$$\sigma_{cr,col} = \frac{n^2 \cdot \pi^2 \cdot E \cdot I}{A \cdot L^2} = \frac{1^2 \cdot \pi^2 \cdot 210000 \frac{N}{mm^2} \cdot 102067938 mm^4}{21818 mm^2 \cdot 6000^2 mm} = 269{,}3\ [MPa]$$

  Comparing the pure column buckling stress to the 2D model result which gave the critical buckling value of 289[MPa], the difference is about 7% which shows that there is some plate like behaviour but it is small. Comparing now to the 3D model ,which gave 315[MPa], to the simple column buckling formula the difference is about 15% which indicates that there is some plate like behaviour going on but still small. A reason for this difference between the 2D and 3D can be assumed to relate to the added stiffness from the weld in the 3D model. The test column results can also be seen in Figure 5.21.

- In panel C the analytical model gave 451[MPa] and EBPlate 424[MPa], which is not far away from double critical buckling strength compared to the FE model results. This clearly indicated that the two methods assume full plate-like-behaviour and therefore overestimate the critical buckling strength drastically.

6 Concluding remarks

In this master thesis global buckling analysis of orthotropic plates was performed with the aim of estimating critical buckling stress. Two type of plates that were included in the thesis where two, stiffened plate with I-stiffeners and a steel sandwich plate with corrugated web. First a thorough literature study of both concepts was conducted before doing parametric studies. For the buckling analysis analytical methods, finite element models and EBPlate were used and then the critical buckling stress between these different methods compared and conclusions drawn from the results. The conclusions observed from the results are stated in the two following subchapters.

6.1 Stiffened plate conclusions

- All methods yield similar results where maximum difference between methods is around 5%.

- For panel D where column like buckling is dominating, all methods are above calculated column buckling stress that indicated that the methods are showing reasonable result.

6.2 SSP conclusions

- Unexpected drop in critical buckling stress was observed when the web thickness was increased in cross-sections 4 and 5 in all panels A, B and C. This drop was not explained but speculations where made which can be seen in chapter 5.4.5.

- A good correlations was observed between both finite element models and EBPlate in panels A and B with cross-sections 1, 2, 3 and 6.

- The analytical method overestimated the critical buckling stress in panels A and B, the overestimation was in the range 4-19% compared to the 3D model results.

- In panel C the analytical method and EBPlate heavily overestimate the critical buckling stress, the overestimation is in the range of 35-72% compared to the 3D model results. From this result it can be concluded that EBPlate and the analytical method both assume full plate like behaviour.

7 Recommendations for future work

In the case of stiffened plates in this master thesis the main focus was on finding analytical methods and working out the finite element modelling. Because a lot more time when into this research there was only time to do a parametric study for stiffened plates with the simplest stiffeners the I-stiffeners. In future studies it would be interesting to do further parametric studies with more variations of stiffeners, for example T-stiffeners and closed-stiffeners. When the stiffeners get more complex effects like torsional stiffness increases which might reveal more difference between the methods.

In the SSP buckling analysis an unexpected drop was observed which we did not manage to explain. Either this drop is the product of wrong modelling technique or that this is an unexplained phenomenon that will break a page in the structural behaviour as we know it for the SSP. Therefore further analysis on this problem would be an interesting addition.

The correlations between EBPlate and the finite element results was an interesting and on some level unexpected observations. The approach that we used to model the SSP in EBPlate was a wild shot that hit the target well according to this small parametric study. A larger parametric study could confirm EBPlate this correlation.

In this master thesis the focus was all on global buckling behaviour of the orthotropic plates. Local buckling is a whole other chapter that has not been research much and would therefore be a logical continues of this work.

The ultimate strength of SSP has also not been researched much taking into account none-linear behaviour, residual stresses, effective are and so forth. This is definitely an interesting research topic and a vital step forward in analysing the behaviour of SSP.

8 References

Abbott, S. P., Systems, P. L., & Caccese, V. (2007). *Automated Laser Welded High Performance Steel Sandwich Bridge Deck Development*.

Alwan, U. L. a, & Järve, D. (2012). *New Concept for Industrial Bridge Construction*.

Beneus, E., & Koc, I. (2014). *Innovative road bridges with steel sandwich decks*. Chalmers.

Chang, W. S., Ventsel, E., Krauthammer, T., & John, J. (2005). Bending behavior of corrugated-core sandwich plates. *Composite Structures*, *70*, 81–89. doi:10.1016/j.compstruct.2004.08.014

Galéa, Y., & Martin, P.-O. (2010). Longitudinally stiffened plates in Eurocode 3: Calculation of the global critical buckling stress. *Journal of Constructional Steel Research*, *66*(11), 1345–1353. doi:10.1016/j.jcsr.2010.05.001

Guo Tong, Li Aiqun, & Li Jianhui. (2008). Fatigue Life Prediction of Welded Joints in Orthotropic Steel Decks Considering Temperature Effect and Increasing Traffic Flow. *Structural Health Monitoring*, *7*, 189–202. doi:10.1177/1475921708090556

Hughes, O. F., Ghosh, B., & Chen, Y. (2004). Improved prediction of simultaneous local and overall buckling of stiffened panels. *Thin-Walled Structures*, *42*(6), 827–856. doi:10.1016/j.tws.2004.01.003

Kolsters, H., & Zenkert, D. (2009). Buckling of laser-welded sandwich panels: ultimate strength and experiments. *Proceedings of the Institution of Mechanical Engineers, Part M: Journal of Engineering for the Maritime Environment*, *224*, 29–45. doi:10.1243/14750902JEME174

Libove, C., & Batdorf, S. B. (1948). A general small deflection theory for flat sandwich plates. *Technical Note 1526. National Advisory Committee for Aeronautics (NACA).*

Libove, C., & Hubka, R. E. (1951). Elastic constants for corrugated-core sandwich plates. *Technical Note 2289, National Advisory Commetee for Aeronautics (NACA).*

Lok, T.-S., & Cheng, Q.-H. (2000). Elastic stiffness properties and behavior of truss-core sandwich panel. *Jurnal of Structural Engineering*, *559*(May), 552–559.

Poirier, J. D., Vel, S. S., & Caccese, V. (2013). Multi-objective optimization of laser-welded steel sandwich panels for static loads using a genetic algorithm. *Engineering Structures*, *49*, 508–524. doi:10.1016/j.engstruct.2012.10.033

Tan, H., Montague, P., & Norris, C. (1989). Steel sandwich panels finite element closed solutions and experimental analysis on a 6x2m panel. *The Structural Engineer*, *67*(9), 159–166.

Timoshenko, S. (1936). *Theory of elastic stability*. NY: McGraw Hill.

Zenkert, D. (1995). *An Itroduction to Sandwich Structures Student Edition* (Second Edi). Stochholm.

Dackman, David & Ek, Walter. (2015). *Utilisation of steel sandwich panels in medium span bridges*. Göteborg: Chalmers University of Technology.

9 Appendix

Geometry and material properties for panel number A4.

Geometry properties

$a := 2000\ mm$	Length of the panel
$b := 2000\ mm$	Width of the panel
$t := 10\ mm$	Thickness of the panel
$h_w := 100\ mm$	Height of stiffener
$t_w := 10\ mm$	Width of stiffener
$n := 10$	Number of stiffeners
$b_{eff} := \frac{b}{n+1} = 181.82\ mm$	Spacing between stiffeners

Material properties and strength parameters

$E := 210000\ MPa$	Young's modulus
$\nu := 0.3$	Poisson's ratio
$G := \frac{E}{2 \cdot (1+\nu)} = (8.077 \cdot 10^4)\ MPa$	Shear modulus
$D := \frac{E \cdot t^3}{12 \cdot (1-\nu^2)} = (1.923 \cdot 10^4)\ J$	Flextural rigidity of isotropic plate
$J_x := \frac{1}{3} \cdot (h_w \cdot {t_w}^3) = (3.333 \cdot 10^4)\ mm^4$	Torsional rigidity

Annex A from EN1993-1-3

Euler buckling stress

$$\sigma_E := \frac{\pi^2 \cdot E \cdot t^2}{12 \cdot (1-\nu^2) \cdot b^2} = 4.745\ MPa$$

Neutral axis and moment of inertia for the panel with all stiffeners

$$y_x := \frac{b \cdot t \cdot \frac{t}{2} + n \cdot \left(h_w \cdot t_w \cdot \left(t + \frac{h_w}{2} \right) \right)}{b \cdot t + n \cdot (h_w \cdot t_w)} = 23.333\ mm$$

$$I_{sl} := \frac{b \cdot t^3}{12} + b \cdot t \cdot \left(\frac{t}{2} - y_x \right)^2 + n \cdot \left(\frac{t_w \cdot h_w^3}{12} + t_w \cdot h_w \cdot \left(-y_x + \frac{h_w}{2} + t \right)^2 \right) = (2.867 \cdot 10^7)\ mm^4$$

$I_p := \frac{b \cdot t^3}{12 \cdot (1-\nu^2)} = (1.832 \cdot 10^5)\ mm^4$ Second moment of area for bending plate

$\gamma := \frac{I_{sl}}{I_p} = 156.52$ Flextural rigidy

$\alpha := \frac{a}{b} = 1$ Aspect ratio

$\psi := 1$ Stress distribution

$A_p := b \cdot t = 0.02\ m^2$ Gross area of the plate

$A_{sl} := n \cdot h_w \cdot t_w = 0.01\ m^2$ Area of stiffeners

$\delta := \frac{A_{sl}}{A_p} = 0.5$ Axial stiffness

$\alpha < \sqrt[4]{\gamma} = 1 \qquad (okay)$

$k_{\sigma.p} := \frac{2 \cdot \left((1+\alpha^2)^2 + \gamma - 1 \right)}{\alpha^2\ (\psi+1) \cdot (1+\delta)} = 106.347$ Buckling coefficient

$\sigma_{cr.p} := k_{\sigma.p} \cdot \sigma_E = 504.62\ MPa$ Critical plate buckling stress

Modified Euler buckling formula (Timoshenko)

$A_T := h_w \cdot t_w + b_{eff} \cdot t = (2.818 \cdot 10^3)\ mm^2$ A_T is the sectional area of a single longitudinal stiffener plus effective plating b_{stiff}.

$A_w := h_w \cdot t_w = (1 \cdot 10^3)\ mm^2$ A_w is the sectional area of stiffener web

Neutral axis and moment of inertia is calculated for effective width of the plate and one stiffener

$$y_x := \frac{b_{eff} \cdot t \cdot \frac{t}{2} + h_w \cdot t_w \cdot \left(t + \frac{h_w}{2}\right)}{b_{eff} \cdot t + h_w \cdot t_w} = 24.516\ mm$$

$$I_x := \frac{b_{eff} \cdot t^3}{12} + b_{eff} \cdot t \cdot \left(\frac{t}{2} - y_x\right)^2 + \frac{t_w \cdot h_w^3}{12} + t_w \cdot h_w \cdot \left(-y_x + \frac{h_w}{2} + t\right)^2 = (2.8001 \cdot 10^6)\ mm^4$$

$I_y := \frac{a \cdot t^3}{12} = (1.667 \cdot 10^5)\ mm^4$ Moment of inertia for I_y

$\rho := \sqrt{\frac{I_x}{A_T}} = 31.521\ mm$ Radius of gyration

$\sigma_E := \frac{\pi^2 \cdot E}{\left(\frac{a}{\rho}\right)^2} = 514.829\ MPa$ Euler column buckling stress

$D_x := \frac{E \cdot I_x}{b_{eff}} = (3.234 \cdot 10^3)\ kN \cdot m$ Flexural rigidity of orthotropic plate in x-direction

$D_y := \frac{E \cdot I_y}{a} = 17.5\ kN \cdot m$ Bending rigidity of orthotropic plate in y-direction

$\Pi_0 := \left(\frac{a}{b}\right) \cdot \left(\frac{D_y}{D_x}\right)^{\frac{1}{4}} = 0.271$ Virtual aspect ratio of orthotropic plate

$H := \frac{G \cdot t^3}{6} + \frac{G \cdot J_x}{b_{eff}} = 28.269\ kN \cdot m$ Torsional rigidity of orthotropic plate

$\eta := \frac{H}{\sqrt{D_x \cdot D_y}} = 0.119$ Torsional stiffness parameter of orthotropic plate

$$\sigma_{ov.panel} := \sigma_E \cdot \left(\frac{A_w \cdot G}{A_w \cdot G + A_T \cdot \sigma_E}\right) \cdot \left(1 + 2 \cdot \eta \cdot \Pi_0^2 + \Pi_0^4\right) = 517.32\ MPa$$

Stiffener's Characteristics

Moment of inertia is calculated for one stiffener plus effective width of the plate.
Effective width is the smaller number of those two:

(A) 20 times the thickness of the plate plus thickness of the stiffener

(B) Width divided with number of spacing between stiffeners

$$b_{eff.1} := 20 \cdot t + t_w = 210 \ mm$$

$$b_{eff.2} := \frac{b}{n+1} = 181.818 \ mm$$

$$b_{eff} := \begin{cases} b_{eff.2} & \text{if } b_{eff.1} \geq b_{eff.2} \\ b_{eff.1} & \text{else} \end{cases}$$

$$b_{eff} = 181.818 \ mm$$

$$y_x := \frac{b_{eff} \cdot t \cdot \frac{t}{2} + h_w \cdot t_w \cdot \left(t + \frac{h_w}{2}\right)}{b_{eff} \cdot t + h_w \cdot t_w} = 24.52 \ mm$$

$$I_x := \frac{b_{eff} \cdot t^3}{12} + b_{eff} \cdot t \cdot \left(y_x - \frac{t}{2}\right)^2 + \frac{t_w \cdot h_w^{\ 3}}{12} + h_w \cdot t_w \cdot \left(-y_x + t + \frac{h_w}{2}\right)^2 = \left(2.8 \cdot 10^6\right) \ mm^4$$

Flextural Stiffness

$$\gamma := \frac{E \cdot I_x}{b \cdot D} = 15.289$$

Torsional stiffness

$$\theta := \frac{G \cdot J_x}{b \cdot D} = 0.07$$

Axial stiffness

$$\delta := \frac{h_w \cdot t_w}{b \cdot t} = 0.05$$

Modified Axial Stiffness

Global buckling can be forced in EBPlate by inserting coefficients to $\eta_x := -1$ ($\beta_x = \beta_x = \eta_y = 0$) and a new modified axial stiffness is calculated.

$\sigma_s := 1\ \boldsymbol{MPa}$

$\sigma_t := 1\ \boldsymbol{MPa}$

$\sigma_b := 1\ \boldsymbol{MPa}$

$\psi_b := \frac{\sigma_s}{\sigma_t} = 1$

$\psi_t := \frac{\sigma_b}{\sigma_s} = 1$

$b_b := b_{eff}$

$b_t := b_{eff}$

$$\delta' := \begin{cases} \delta + \left(\frac{3-\psi_t}{5-\psi_t} \cdot \frac{b_t}{b} + \frac{2}{5-\psi_b} \cdot \frac{b_b}{b}\right) & \text{if } \psi_b \geq 0 \\ \delta + \left(\frac{3-\psi_t}{5-\psi_t} \cdot \frac{b_t}{b} + \frac{2}{5-\psi_b} \cdot \frac{b_b}{b}\right) & \text{else} \end{cases}$$

$\delta' = 0.141$

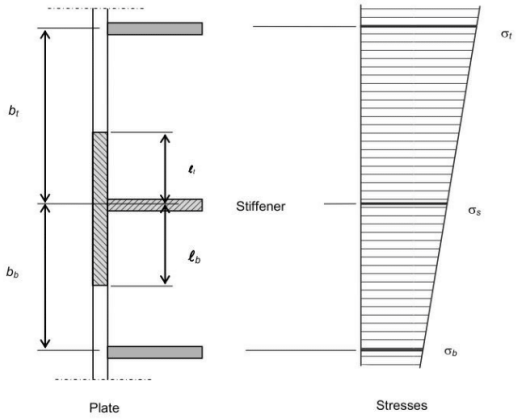

Figure: (Galéa & Martin, 2010)

Orthotropic coefficiants

Moment of inertia is calculated for one stiffener plus effective width of the plate.
Effective width is the smaller number of those two:

(A) 20 times the thickness of the plate plus thickness of the stiffener

(B) Width divided with number of spacing between stiffeners

$$b_{eff.1} := 20 \cdot t + t_w = 210 \ mm$$

$$b_{eff.2} := \frac{b}{n+1} = 181.818 \ mm$$

$$b_{eff} := \begin{cases} b_{eff.2} & \text{if } b_{eff.1} \geq b_{eff.2} \\ b_{eff.1} & \text{else} \end{cases}$$

$$b_{eff} = 181.818 \ mm$$

$$y_x := \frac{b_{eff} \cdot t \cdot \frac{t}{2} + h_w \cdot t_w \cdot \left(t + \frac{h_w}{2}\right)}{b_{eff} \cdot t + h_w \cdot t_w} = 24.52 \ mm$$

$$I_x := \frac{b_{eff} \cdot t^3}{12} + b_{eff} \cdot t \cdot \left(y_x - \frac{t}{2}\right)^2 + \frac{t_w \cdot h_w^3}{12} + h_w \cdot t_w \cdot \left(-y_x + t + \frac{h_w}{2}\right)^2 = \left(2.8 \cdot 10^6\right) \ mm^4$$

Flexural rigidity of orthotropic plate in x-direction

$$D_x := \frac{E \cdot (n+1) \cdot I_x}{b} = \left(3.234 \cdot 10^3\right) \ kN \cdot m$$

change of transverse flexural plate rigidity

$$\beta_x := \frac{D_x}{D} - 1 = 167.174$$

Area of the section (effective width plus the stiffener)

$$A_x := b_{eff} \cdot t + h_w \cdot t_w = 0.003 \ m^2$$

change of transverse area, with the respect to the reference plate area.

$$\eta_x := \frac{A_x}{b_{eff} \cdot t} - 1 = 0.55$$

Stiffness parameters

Table 1. Stiffness parameters for 6x2.1m panel comparing current and Chengs results.

Panel nr.	Study	D_x [Nm]	D_y [Nm]	D_{xy} [Nm]	D_{Qx} [N/m]	D_{Qy} [N/m]
A1	*Cheng*	*1,32E+07*	*1,13E+07*	*8,56E+06*	*3,48E+08*	*3,47E+07*
	Current	*1,32E+07*	*1,13E+07*	*8,56E+06*	*3,257E+08*	*2,954E+07*
A2	*Cheng*	*1,33E+07*	*1,13E+07*	*8,56E+06*	*2,63E+08*	*1,43E+07*
	Current	*1,33E+07*	*1,13E+07*	*8,56E+06*	*2,41E+08*	*1,22E+07*
A3	*Cheng*	*1,34E+07*	*1,13E+07*	*8,56E+06*	*2,06E+08*	*8,74E+06*
	Current	*1,34E+07*	*1,13E+07*	*8,56E+06*	*1,86E+08*	*6,63E+06*
A4	*Cheng*	*8,39E+06*	*6,44E+06*	*4,84E+06*	*3,28E+08*	*2,45E+07*
	Current	*8,39E+06*	*6,44E+06*	*4,84E+06*	*3,07E+08*	*2,07E+07*
A5	*Cheng*	*8,48E+06*	*6,44E+06*	*4,84E+06*	*2,48E+08*	*1,02E+07*
	Current	*8,48E+06*	*6,44E+06*	*4,84E+06*	*2,27E+08*	*9,05E+06*
A6	*Cheng*	*8,54E+06*	*6,44E+06*	*4,84E+06*	*1,94E+08*	*5,66E+06*
	Current	*8,54E+06*	*6,44E+06*	*4,84E+06*	*1,75E+08*	*5,10E+06*
A7	*Cheng*	*7,04E+06*	*5,08E+06*	*3,80E+06*	*3,22E+08*	*2,15E+07*
	Current	*7,04E+06*	*5,08E+06*	*3,80E+06*	*3,01E+08*	*1,81E+07*
A8	*Cheng*	*7,13E+06*	*5,08E+06*	*3,80E+06*	*2,43E+08*	*9,34E+06*
	Current	*7,13E+06*	*5,08E+06*	*3,80E+06*	*2,23E+08*	*8,13E+06*
A9	*Cheng*	*7,19E+06*	*5,09E+06*	*3,80E+06*	*1,91E+08*	*5,14E+06*
	Current	*7,19E+06*	*5,09E+06*	*3,80E+06*	*1,72E+08*	*4,64E+06*
A10	*Cheng*	*1,37E+07*	*1,13E+07*	*8,56E+06*	*3,32E+08*	*1,07E+07*
	Current	*1,37E+07*	*1,13E+07*	*8,56E+06*	*3,02E+08*	*8,64E+06*
A11	*Cheng*	*1,37E+07*	*1,13E+07*	*8,56E+06*	*2,52E+08*	*5,99E+06*
	Current	*1,37E+07*	*1,13E+07*	*8,56E+06*	*2,25E+08*	*4,98E+06*
A12	*Cheng*	*1,37E+07*	*1,13E+07*	*8,56E+06*	*1,98E+08*	*3,89E+06*
	Current	*1,37E+07*	*1,13E+07*	*8,56E+06*	*1,75E+08*	*3,27E+06*
A13	*Cheng*	*8,87E+06*	*6,46E+06*	*4,84E+06*	*3,13E+08*	*8,17E+06*
	Current	*8,87E+06*	*6,46E+06*	*4,84E+06*	*2,85E+08*	*6,77E+06*
A14	*Cheng*	*8,87E+06*	*6,46E+06*	*4,84E+06*	*2,37E+08*	*4,78E+06*
	Current	*8,87E+06*	*6,46E+06*	*4,84E+06*	*2,12E+08*	*4,03E+06*
A15	*Cheng*	*8,88E+06*	*6,46E+06*	*4,84E+06*	*1,87E+08*	*3,14E+06*
	Current	*8,88E+06*	*6,46E+06*	*4,84E+06*	*1,65E+08*	*2,70E+06*
A16	Cheng	7,52E+06	5,10E+06	3,80E+06	3,07E+08	7,79E+06
	Current	7,52E+06	5,10E+06	3,80E+06	2,80E+08	6,20E+06
A17	Cheng	7,52E+06	5,10E+06	3,80E+06	2,33E+08	5,92E+06
	Current	7,52E+06	5,10E+06	3,80E+06	2,08E+08	3,73E+06
A18	Cheng	7,53E+06	5,10E+06	3,80E+06	1,83E+08	2,96E+06
	Current	7,53E+06	5,10E+06	3,80E+06	1,62E+08	2,52E+06
A19	Cheng	1,42E+07	1,14E+07	8,56E+06	3,13E+08	5,02E+06
	Current	1,42E+07	1,14E+07	8,56E+06	2,79E+08	3,82E+06
A20	Cheng	1,41E+07	1,14E+07	8,56E+06	2,39E+08	3,37E+06
	Current	1,41E+07	1,14E+07	8,56E+06	2,10E+08	2,62E+06

A21	Cheng	1,40E+07	1,13E+07	8,56E+06	1,89E+08	2,43E+06
	Current	1,40E+07	1,13E+07	8,56E+06	1,64E+08	1,93E+06
A22	Cheng	9,31E+06	6,48E+06	4,84E+06	2,95E+08	4,15E+06
	Current	9,31E+06	6,48E+06	4,84E+06	2,63E+08	3,26E+06
A23	Cheng	9,24E+06	6,48E+06	4,84E+06	2,25E+08	2,86E+06
	Current	9,24E+06	6,48E+06	4,84E+06	1,98E+08	2,26E+06
A24	Cheng	9,19E+06	6,48E+06	4,84E+06	1,78E+08	2,11E+06
	Current	9,19E+06	6,48E+06	4,84E+06	1,54E+08	1,67E+06
A25	Cheng	7,96E+06	5,12E+06	3,80E+06	2,90E+08	4,05E+06
	Current	7,96E+06	5,12E+06	3,80E+06	2,58E+08	3,09E+06
A26	Cheng	7,89E+06	5,12E+06	3,80E+06	2,21E+08	2,74E+06
	Current	7,89E+06	5,12E+06	3,80E+06	1,94E+08	2,15E+06
A27	Cheng	7,84E+06	5,11E+06	3,80E+06	1,75E+08	1,99E+06
	Current	7,84E+06	5,11E+06	3,80E+06	1,52E+08	1,59E+06

Panel nr.	Study	Cheng deflection [mm]	Analytical deflection [mm]	FEM deflection [mm]	Analytical Vs 2D FEM [%]	Cheng Vs Current [%]
A1	Cheng	0,338	0,3375	0,3378	-0,09%	
	Current		0,3622	0,3627	-0,14%	-6,84%
A2	Cheng	0,536	0,5337	0,5345	-0,15%	
	Current		0,5885	0,5895	-0,17%	-9,32%
A3	Cheng	0,732	0,7306	0,7319	-0,18%	
	Current		0,8801	0,8818	-0,19%	-16,99%
A4	Cheng	0,547	0,5466	0,547	-0,07%	
	Current		0,5837	0,5842	-0,09%	-6,36%
A5	Cheng	0,823	0,8232	0,824	-0,10%	
	Current		0,8814	0,8822	-0,09%	-6,60%
A6	Cheng	1,18	1,1764	1,178	-0,14%	
	Current		1,2593	1,261	-0,13%	-6,58%
A7	Cheng	0,67	0,6689	0,6693	-0,06%	
	Current		0,7124	0,7128	-0,06%	-6,10%
A8	Cheng	0,964	0,9639	0,9646	-0,07%	
	Current		1,0391	1,04	-0,09%	-7,24%
A9	Cheng	1,36	1,3626	1,364	-0,10%	
	Current		1,4541	1,456	-0,13%	-6,31%
A10	Cheng	0,64	0,6385	0,6392	-0,11%	
	Current		0,7341	0,735	-0,12%	-13,03%
A11	Cheng	0,94	0,9392	0,9405	-0,14%	
	Current		1,0649	1,067	-0,20%	-11,83%
A12	Cheng	1,26	1,2578	1,26	-0,17%	
	Current		1,4116	1,414	-0,17%	-10,89%
A13	Cheng	0,935	0,9346	0,9353	-0,07%	
	Current		1,048	1,049	-0,10%	-10,83%
A14	Cheng	1,31	1,3103	1,311	-0,05%	-10,73%

	Current		1,4673	1,469	-0,12%	
A15	Cheng	1,74	1,7337	1,736	-0,13%	
	Current		1,9186	1,921	-0,13%	-9,63%
A16	Cheng	1,06	1,0627	1,063	-0,03%	
	Current		1,2131	1,214	-0,07%	-12,42%
A17	Cheng	1,25	1,2478	1,249	-0,10%	
	Current		1,6706	1,672	-0,08%	-25,30%
A18	Cheng	1,95	1,9459	1,948	-0,11%	
	Current		2,1661	2,168	-0,09%	-10,16%
A19	Cheng	1,06	1,0537	1,055	-0,12%	
	Current		1,2642	1,266	-0,14%	-16,66%
A20	Cheng	1,38	1,3746	1,376	-0,10%	
	Current		1,6137	1,616	-0,14%	-14,83%
A21	Cheng	1,7	1,694	1,696	-0,12%	
	Current		1,9446	1,948	-0,17%	-12,91%
A22	Cheng	1,44	1,4341	1,435	-0,06%	
	Current		1,6833	1,685	-0,10%	-14,82%
A23	Cheng	1,84	1,8366	1,84	-0,19%	
	Current		2,1463	2,148	-0,08%	-14,38%
A24	Cheng	2,25	2,2466	2,249	-0,11%	
	Current		2,6077	2,611	-0,13%	-13,86%
A25	Cheng	1,58	1,5788	1,58	-0,08%	
	Current		1,8834	1,884	-0,03%	-16,15%
A26	Cheng	2,04	2,0405	2,042	-0,07%	
	Current		2,3943	2,396	-0,07%	-14,78%
A27	Cheng	2,52	2,5212	2,523	-0,07%	
	Current		2,9147	2,912	0,09%	-13,43%